U.S. DEPARTMENT OF COMMERCE
National Technical Information Service

PB-255 093

OPTICAL METHOD FOR MEASURING THE MASS CONCENTRATION OF PARTICULATE EMISSIONS

METEOROLOGY RESEARCH, INCORPORATED

PREPARED FOR
ENVIRONMENTAL SCIENCES RESEARCH LABORATORY

MARCH 1976

209113

EPA-600/2-76-062
March 1976

PB 255 093

Environmental Protection Technology Series

REPRODUCED BY
NATIONAL TECHNICAL
INFORMATION SERVICE
U. S. DEPARTMENT OF COMMERCE
SPRINGFIELD, VA. 22161

TECHNICAL REPORT DATA
(Please read Instructions on the reverse before completing)

1. REPORT NO. EPA-600/2-76-062	2.
3. RECIPIENT'S ACCESSION NO. PB255093	
4. TITLE AND SUBTITLE: OPTICAL METHOD FOR MEASURING THE MASS CONCENTRATION OF PARTICULATE EMISSIONS	5. REPORT DATE: March 1976
	6. PERFORMING ORGANIZATION CODE
7. AUTHOR(S): Gregory R. Markowski, George J. Woffinden and David S. Ensor	8. PERFORMING ORGANIZATION REPORT NO.: MRI 75 FR-1379
9. PERFORMING ORGANIZATION NAME AND ADDRESS: Meteorology Research, Inc. 464 W. Woodbury Road Altadena, California 91001	10. PROGRAM ELEMENT NO.: 1AA010
	11. CONTRACT/GRANT NO.: 68-02-1749
12. SPONSORING AGENCY NAME AND ADDRESS: Environmental Sciences Research Laboratory Office of Research and Development U. S. Environmental Protection Agency Research Triangle Park, N. C. 27711	13. TYPE OF REPORT AND PERIOD COVERED: final
	14. SPONSORING AGENCY CODE: EPA - ORD
15. SUPPLEMENTARY NOTES	

16. ABSTRACT

The objective of this study is to demonstrate the feasibility of an in-situ across-the-stack optical technique to measure the mass of particulate emissions from stationary sources. The technique uses small angle light scattering and transmittance to determine a quantity closely related to particulate mass concentration. The forward scattered light is measured at an angle of 1° or less.

The technique has been investigated both theoretically using Mie theory, and experimentally using aerosols produced in the laboratory. The experimental results agree with the theoretical predictions and indicate that the method is relatively insensitive to changes in aerosol parameters such as particle size, refractive index, and shape.

17. KEY WORDS AND DOCUMENT ANALYSIS

a. DESCRIPTORS	b. IDENTIFIERS/OPEN ENDED TERMS	c. COSATI Field/Group
Optical measuring instruments		14B
*Transmittance		20F
*Light scattering		13B
Air pollution		07D
*Aerosols		14G
*Weight (mass)		

18. DISTRIBUTION STATEMENT: RELEASE TO PUBLIC	19. SECURITY CLASS (This Report): UNCLASSIFIED	21. NO. OF PAGES: 96
	20. SECURITY CLASS (This page): UNCLASSIFIED	22. PRICE: 5.00

EPA Form 2220-1 (9-73)

OPTICAL METHOD FOR MEASURING THE MASS CONCENTRATION OF PARTICULATE EMISSIONS

by

Gregory R. Markowski
George J. Woffinden
David S. Ensor
Meteorology Research, Inc.
Altadena, California 91001

Contract No. 68-02-1749

Project Officer
William Conner

Emission Measurement and Characterization Division
Environmental Sciences Research Laboratory
Research Triangle Park, N.C. 27711

U.S. ENVIRONMENTAL PROTECTION AGENCY
OFFICE OF RESEARCH AND DEVELOPMENT
ENVIRONMENTAL SCIENCES RESEARCH LABORATORY
RESEARCH TRIANGLE PARK, NORTH CAROLINA 27711

12

Disclaimer

This report has been reviewed by the Environmental Sciences Research Laboratory, U.S. Environmental Protection Agency, and approved for publication. Approval does not signify that the contents necessarily reflect the views and policies of the U.S. Environmental Protection Agency, nor does mention of trade names or commercial products constitute endorsement or recommendation for use.

ABSTRACT

The objective of this study is to demonstrate feasibility of an in situ across-the-stack optical technique for the mass measurement of particulate emissions from stationary sources. The technique uses small angle light scattering and transmittance to determine a quantity closely related to particulate mass concentration. The forward scattered light is measured at an angle of 1° or less.

The technique has been investigated both theoretically using Mie theory, and experimentally using aerosols produced in the laboratory. The experimental results agree with the theoretical predictions and indicate that the method is relatively insensitive to changes in aerosol parameters such as particle size, refractive index, and shape.

CONTENTS

		Page
Abstract		v
List of Figures		ix
List of Tables		xi
Nomenclature		xii
Sections		
1	CONCLUSIONS	1
2	RECOMMENDATIONS	2
3	INTRODUCTION	4
4	SCATOMETER THEORY	6
	Theory of Scatometer Algorithm	6
	Modeling Calculations	8
	Monodisperse Aerosol Calculations	9
	Polydisperse Aerosol Calculations	16
	Correction Techniques	24
	Active Volume Considerations	26
5	EXPERIMENTAL STUDIES	31
	Experimental Design	31
	Initial Experimental Apparatus	31
	Aerosol Generation	36
	Revised Scatometer Design	37
	Recommendations for Optical Design Improvement	40

CONTENTS (continued)

	Page
Scatometer Experiments	46
Experimental Data Normalization	46
Experiments, Set 1	46
Experiments, Set 2	48
Experimental Results	48
6 REFERENCES	65
Appendix A - Experimental Data Logs	67
Appendix B - Data Reduction Computations	84

FIGURES

No.		Page
1	Predicted Scatometer Response Per Unit Volume of Typical Aerosols as a Function of Particle Size	13
2	Predicted Scatometer Response Per Unit Volume of Aerosol as a Function of Particle Size and Changes in Refractive Index	14
3	Predicted Scatometer Response Per Unit Volume of Aerosol as a Function of Particle Size and Various Scattering Angles	15
4	Predicted Scatometer Response Per Unit Volume of Aerosol as a Function of the Size Parameters of Lognormal Volume Distributions, $\theta = 0.5^{\circ}$	19
5	Predicted Scatometer Response Per Unit Volume of Aerosol as a Function of the Size Parameters of Lognormal Volume Distributions, $\theta = 1^{\circ}$	20
6	Predicted Transmissometer Response Per Unit Volume of Aerosol as a Function of the Size Parameters of Lognormal Volume Distributions	21
7	Comparison of Predicted Scatometer and Transmissometer Response Per Unit Volume of Aerosol as a Function of the Size Parameters of Lognormal Volume Distributions for Carbon	22
8	Corrected Scatometer Response Per Unit Volume of Aerosol as a Function of the Size Parameters of Lognormal Volume Distributions	25
9	Active Scattering Volume	27
10	Diagram of Optical Arrangement for Initial Scattering-Opacity Experiments	32
11	Light Image in the Scatometer Focal Plane with no Aerosol Present	33

FIGURES (continued)

		Page
12	Light Image in the Scatometer Focal Plane with a Simulated Aerosol in the Beam	35
13	Diagram of Aerosol Generator	38
14	Scatometer Diagram	39
15	Scatometer and Aerosol Test Chamber	41
16	Detector and Crossfeed Mounting	43
17	Scatometer Light Source	45
18	Experimental Scatometer Response Per Unit Mass Concentration of Aerosol as a Function of Particle Size	52
19	Relative Experimental Transmissometer Response (Optical Depth Per Unit Mass Concentration ofAerosol) as a Function of Particle Size	53
20	Experimental Scatometer Response Per Predicted Response as a Function of Particle Size	55
21	Polystyrene Latex Aerosol Particles, 1/2 μm Diameter	56
22	Polyvinyltoluene Latex Aerosol Particles, 2 μm Diameter	57
23	Ammonium Fluorescein Aerosol Particles, 0.57 μm Volume Median Diameter	59
24	Ammonium Fluorescein Aerosol Particles, 3 μm Diameter, Experimental Set 1	61
25	Ammonium Fluorescein Aerosol Particles, 2.8 μm Diameter, Experimental Set 2	63
A-1	Set 1, Test 1 Aerosol SEM Photomicrograph	68

TABLES

No.		Page
1	Parameter Ranges for Scatometer Response Calculations	10
2	Active Volume and Active Volume Ratios	29
3	Active Volume Ratios for Current Scatometer Geometry	30
4	Size Distributions to Show Scatometer Feasibility	47
5	Scatometer Experimental Results, Set 1	49
6	Scatometer Experimental Results, Set 2	50

NOMENCLATURE

λ	=	light wavelength
$\eta(r)$	=	size distribution
ρ	=	aerosol specific gravity
$\sigma(\theta)$	=	total angular scattering cross section of aerosol in Scatometer beam
σ_e	=	total extinction cross section of aerosol in Scatometer beam
σ_g	=	geometric standard deviation
θ	=	scattering angle
A	=	active area
A_b	=	area of Scatometer beam
b	=	aerosol scattering coeffici nt
b_N	=	scattering coefficient at reference relative aerosol density
C_o	=	$(k/2)\sqrt{\pi Q_o}$
d	=	aerosol particle parameter
d_g	=	geometric mean diameter, also volume median diameter as used in the text
D	=	aerosol chamber length
D_s	=	distance from lens to aerosol chamber
I	=	beam intensity after attentuation by aerosol
I_o	=	beam intensity before attentuation by aerosol
k	=	$2\pi / \lambda$
l	=	path length of transmittance measurement

L	=	length of Scatometer chamber
m	=	index of refraction
M	=	aerosol mass concentration determined gravimetrically by filtration
M_N	=	M normalized to constant aerosol density using b_N
$M_s(\theta)$	=	Scatometer mass, $\rho V(\theta)$
N	=	number of particles in Scatometer beam
N_o	=	normalization constant
O	=	optical depth
O_N	=	optical depth normalized to constant aerosol density
$P(\theta)$	=	power received by detector at scattering angle θ
P_B	=	beam power during measurement of $P(\theta)$
P_{BN}	=	Scatometer beam strength to which all intensity measurements in an experiment are normalized.
$P_N(\theta)$	=	$P(\theta)$ normalized to P_{BN}
$P'_N(\theta)$	=	$P_N(\theta)$ corrected by the active volume ratio
$P_{NO}(0)$	=	normalized transmitted beam power without aerosol
Q	=	extinction efficiency factor
Q_o	=	approximate extinction efficiency factor
$R(\theta)$	=	ratio of active to total beam volume at scattering angle, θ
r	=	aerosol radius
r_D	=	radius of detector aperture
r_f	=	focal length of focusing lens
$r_s(\theta)$	=	radius from beam focal point at which light scattered at angle θ is focused

r_{max}	=	upper size limit for computational size distributions
r_{min}	=	lower size limit for computational size distributions
R_B	=	beam radius
R_L	=	lens radius
T	=	transmittance
T_N	=	T normalized to B_N
V	=	true volume of aerosol in Scatometer beam
$V(\theta)$	=	volume of aerosol in Scatometer beam determined using light scattered at angle θ
V_A	=	active volume
$V_c(\theta)$	=	aerosol volume concentration determined by Scatometer using scattered light at angle θ
x_i	=	a measured value

SECTION 1

CONCLUSIONS

Both the theoretical and experimental work performed indicate that the Scatometer technique (combined scattering and transmittance) provides an in situ optical method for aerosol mass measurement that is relatively unaffected by changes in aerosol parameters such as particle size, refractive index, and shape. The relative insensitivity of the method to changes in aerosol parameters provides an improvement over the transmissometer for monitoring the mass concentration of sources with time variable aerosol parameters.

Scatometer modeling results indicate that errors in measuring aerosol volume will not exceed $\pm$ 30 percent for changes in volume median diameters from 0.5 to 10 μm and for wide changes in polydispersity or refractive index. An initial calibration to correlate aerosol volume to aerosol mass will likely reduce these error limits. Additional correction methods have been investigated which indicate a potential accuracy of $\pm$ 15 percent for aerosol volume determination.

The theoretical predictions, which have been confirmed by experiment, indicate that the Scatometer technique will be a considerable improvement over a transmissometer for monitoring aerosols whose size distributions or refractive index vary significantly.

The experimental work indicates that the Scatometer algorithm performs in the laboratory as predicted by theory and shows insensitivity to particle size, shape, and refractive index. The experimental work indicates that the theoretical model based on Mie theory is a good predictor of Scatometer performance on field aerosols.

SECTION 2

RECOMMENDATIONS

The completed experimental and theoretical work both show that the Scatometer approach is simple and effective for accurate measurements of aerosol mass concentrations. Because of the success of these preliminary results, the following steps are strongly recommended for further development of the Scatometer:

1. Improved accuracy in Scatometer mass measurements can be provided by simultaneously monitoring scattering intensity at more than one angle. Each additional intensity measured should further improve the accuracy of mass determinations. Experimental evaluations are required to verify the magnitude of these improvements. A cost vs accuracy trade-off analysis can then be made.

2. Field evaluation of the Scatometer is required to demonstrate performance with "real world" aerosols. Preliminary performance evaluations are recommended at the EPA "stack simulator" wind tunnel. These evaluations will provide maximum control and characterization of test aerosols.

3. Following the simulated stack tests, the Scatometer should be evaluated in the field on industrial emission sources. These evaluations will demonstrate the effects of vibration, elevated temperature, and soiling of optical elements. They will also show the improvement in mass measurements that can be obtained over the transmissometer when aerosol properties change as a result of boiler process variations.

4. The Scatometer can be made insensitive to vibration and beam wander by using an array of solid state detectors (rather than a single detector as used in the laboratory prototype). An electronic coincidence circuit will allow data to be recorded only when the optical axis of the Scatometer beam is centered on the detector array. Such a detector array can measure scattering intensities simultaneously at several scattering angles.

5. Scatometer retrofit kits should be considered for converting standard transmissometers into Scatometers. Conversion of existing plant instruments could provide the plant operator

with additional control data at a minimum cost. The Scatometer represents a very promising method for improving accuracy of stack aerosol mass measurements.

SECTION 3

INTRODUCTION

Monitoring particulate mass emissions from stationary sources such as coal-fired boiler stacks is currently one of the nation's important environmental problems. A number of mass measurement instruments have been developed, such as the piezoelectric microbalance and beta radiation gauge; however, they require (1) sample removal from the stack and, therefore, suffer from resulting errors, and (2) exposure of a section of the instrument to the hostile stack environment.

Transmissometers have been used to determine in-stack optical density, and this quantity has been linearly correlated to the mass concentration. Optical methods have the important advantages of (1) real-time in situ measurement, (2) across-the-stack averaging, and (3) isolation of sensors from the stack environment. The serious disadvantage of the transmissometer is that the measured quantity, transmittance, is not only a function of the mass or volume of the aerosol, but also the refractive index and particle size. Therefore, accurate measurements of mass are difficult unless refractive index and particle size are reasonably constant.

The Scatometer technique (combined forward scattering and transmittance) investigated in this contract is designed to retain the advantages of the transmissometer method and to determine a quantity more closely related to aerosol volume and much less dependent on refractive index and particle size.

The objective of the work performed under this contract is to determine feasibility of the Scatometer technique for measuring particulate mass emissions from stationary sources, such as coal- and oil-fired boilers.

The program has been divided into two main parts: (1) theoretical and (2) experimental work.

The primary goals of the theoretical work are three-fold:

(1) To predict the Scatometer response for typical stack aerosols which are normally not producible in the laboratory.

(2) To indicate expected accuracy of Scatometer mass measurements and to show where further development is needed.

(3) To form a basis for comparison with the transmissometer and other stack monitoring methods.

The primary goals of the experimental work are two-fold:

(1) To determine how accurately Scatometer techniques can determine aerosol mass concentrations under laboratory conditions.

(2) To determine how well the experimental response agrees with theory.

Because laboratory experimental results have verified the theoretical model predictions, the Scatometer is expected to measure stack aerosols more accurately than other currently available stack monitoring systems.

SECTION 4

SCATOMETER THEORY

A number of researchers, among them Shifrin[1], Gunther[2], and Livesey[3] have investigated light scattering to determine aerosol size distribution, volume, or particle size. These authors have used diffraction and Rayleigh Gans approximations for calculating forward light scattering. Meehan and Gyberg[4] have investigated refractive index effects with the Mie equations. The Scatometer technique estimates aerosol volume, and hence mass concentration, by using the extinction and the near forward angular scattering cross sections. It is based on two approximations: the diffraction approximation for light scattered in the near forward direction, and an extinction approximation for estimating the aerosol optical extinction cross section. The technique is insensitive to size distribution and refractive index over a wide range of parameters. Implementation of the technique appears practical since only two scattering parameters need be measured: the forward scattered intensity and the optical depth (extinction cross section).

THEORY OF SCATOMETER ALGORITHM

For an aerosol particle radius, r , sufficiently large, and scattering angle, θ, sufficiently small, the angular scattering cross section for a single particle, $\sigma_p(\theta)$, is accurately given by the diffraction approximation as

$$\sigma_p(\theta) = \frac{r^2 J_1^2 (k r \theta)}{\theta^2} \qquad (1)$$

where k is the wave number, $2\pi/\lambda$; J_1 is the first order Bessel function; θ is the scattering angle; r is the particle radius; and p denotes a single particle. For the product $(kr\theta)$ less than 1, this equation can be reasonably approximated for this purpose by its lowest order term:

$$\sigma_p(\theta) \cong k^2 r^4/4 \qquad (2)$$

Thus, for a sufficiently small angle, θ, depending on λ and r, the scattering is independent of the scattering angle and dependent on the fourth power of the radius. Because of the independence of angle,

the near forward scattering cross section for a distribution of particles, $\sigma(\theta)$, can be expressed as

$$\sigma(\theta) \cong N k^2 \overline{r^4}/4 \tag{3}$$

where $\overline{r^4}$ is the arithmetic average of r^4 over the aerosol size distribution and N is the number of scattering particles. The total angular cross section is obtained in practice by determining the total power, P, scattered at a given angle per steradian from a collimated beam of light and dividing by the intensity of the emerging beam, I:

$$\sigma(\theta) = P(\theta)/I \tag{4}$$

Secondly, the extinction cross section, σ_e, for the aerosol is given by

$$\sigma_e = \pi N \overline{Q(r/\lambda, m) r^2} \tag{5}$$

where the bar denotes the arithmetic average over the aerosol distribution. $Q(r/\lambda, m)$ is the scattering efficiency factor and m is the index of refraction. The extinction cross section, σ_e, is usually determined using the ratio of the beam intensity before and after passing through the aerosol and the following formula derived from Beer's law: $I/I_o = \exp(-\sigma_e/A_b)$ where I_o is the intensity of the incident beam, and A_b is its area. σ_e/A_b is the optical depth and is equal to bl in Beer's law: $I/I_o = e^{-bl}$ where b is the aerosol extinction coefficient and l is the measurement path length.

For r sufficiently large, generally greater than 2λ, an extinction approximation can be made with reasonable accuracy by assuming that $Q(r/\lambda, m)$ is a constant, Q_o. From Equation (5) then

$$\sigma_e \cong \pi Q_o N \overline{r^2} \tag{6}$$

Taking the square root of the product $\sigma(\theta)$ (σ_e) gives

$$\sqrt{\sigma_\theta \, \sigma_e} \cong C_o N \sqrt{\overline{r^2} \; \overline{r^4}} \tag{7}$$

where $C_o = (k/2)\sqrt{\pi Q_o}$. The square root on the right of Equation (7) can be reasonably well approximated by the following:

$$\sqrt{\overline{r^2}\ \overline{r^4}} \cong \overline{r^3} \tag{8}$$

and Equation (7) becomes

$$\sqrt{\sigma(\theta)\,\sigma_e} \cong C_o N \overline{r^3} \tag{9}$$

Equation (9) indicates that the square root on the left side is directly proportional to the aerosol's volume. Noting that the total aerosol volume, V, in the beam is given by $4/3\ \pi N \overline{r^3}$ and using Equation (9) to solve for V, the desired relationship is obtained:

$$V \cong \frac{4\pi}{3 C_o} \sqrt{\sigma(\theta)\,\sigma_e} \tag{10}$$

This result is the basis of the Scatometer technique and indicates that aerosol volume in a beam can be determined by measuring the total forward scattering and total extinction cross sections. Furthermore, the result will be insensitive to the shape of the size distribution since the error inherent in Equation (8) is neither large nor highly variable with respect to size distribution shape.

The important approximations used in deriving Equation (10), Equations (3) and (6), are known to be accurate for particles larger than 2 to 4 μm in diameter. The next step in the analysis determined the true cross sections using Mie theory to permit accurate response characterization for both large and small particles and various forward scattering angles.

MODELING CALCULATIONS

The objective of the modeling calculations was to determine the range of validity of forward scattering and extinction approximations, Equations (2) and (6), and more importantly the actual response of the technique, Equation (10), for various parameters. The technique was modeled on a CDC 6400 computer using the Mie equations to calculate the forward scattering and extinction cross sections for spherical particles[5]. The calculations were divided into two areas: monodisperse and polydisperse (lognormal) size distributions. The monodisperse calculations permitted

a detailed examination of the response of the technique over a wide range of particle sizes, indices of refraction and forward scattering angles. These results were then averaged over a wide range of lognormal size distributions to model expected response for stack aerosols and the experimental work. Calculations of extinction cross sections was a necessary part of the calculations and permitted easy comparison between Scatometer and transmissometer response.

Monodisperse Aerosol Calculations

To obtain Scatometer response for monodisperse aerosols, the forward scattering and extinction cross sections were computed for narrow rectangular size distributions, $\eta(r)$, of unit volume as defined below:

$$\eta(r) = N_o \text{ for } r_{min} \leq r \leq r_{max}$$

$$\eta(r) = 0 \quad \text{otherwise} \tag{11}$$

and $$r_{max}/r_{min} = 1.2$$

N_o is defined such that the total aerosol volume is equal to one:

$$\int_o^\infty \eta(r)\,(4/3)\,\pi\,r^3\,dr = 1 \tag{12}$$

These narrow size distributions were used instead of discrete points to average the fluctuations of the Mie solutions, thus facilitating plotting and interpretation of the data obtained. The averaging is desirable since the polydisperse aerosols encountered in the field will not reflect the fine structure of Mie solutions. Since the size distributions are initially normalized to unit volume, the volume computed by the Scatometer algorithm, Equation (10), is a response ratio, the Scatometer volume divided by the true volume, and is a function of the aerosol parameters and forward scattering angle. The integrations over the size distributions were performed using Romberg integration, an adaptive technique (Davis and Rabinowitz[6] and Ralston and Wiff[7]). The algorithm convergence parameters were adjusted to limit the error to 6 percent with about 95 percent confidence. Inspection of the integration routine output indicated that most quadratures were accurate to 2 percent. A number of cases were run with smaller error tolerances to guide the final convergence parameters. Response calculations were performed for the combinations of parameters presented in Table 1. A number of refractive indices

Table 1. PARAMETER RANGES FOR SCATOMETER RESPONSE CALCULATIONS

GROUP	REFRACTIVE INDEX	MATERIAL	SIZE RATIO, r/λ, RANGE	FORWARD SCATTERING ANGLE (DEGREES)
1	1.333	Water	0.05 - 20	0, 1/2, 1, 2
	1.5	Fly Ash		
	1.6	Polystyrene		
	1.5 - 0.02 i	Absorptive Fly Ash	0.05 - 10	4, 7, 10
	1.96 - 0.66 i	Amorphous Carbon (Soot)		
2	1.45		0.05 - 4.68	1/2, 1, 2
	1.55			
	1.45 - 0.02 i			
	1.55 - 0.02 i			
	1.91 - 0.66 i			
	2.01 - 0.66 i			
3	1.5	Fly Ash	0.031 - 63.6*	1/2
	1.6	Polystyrene		
	1.34 - 0.02 i	Absorptive Water	0.031 - 36.9*	1
	1.75 - 0.02 i	Ammonium Fluorescein		
	1.96 - 0.66 i	Amorphous Carbon		

* Lower size for carbon was 0.008 microns

were used which represent substances commonly found in coal- and oil-fired boiler emissions. The refractive indices in Group 2, Table 1, were used to check the sensitivity of the technique to small changes in refractive index. The angles $1/2^{\circ}$ and up were chosen to test those which may be useful in a practical instrument. Zero degrees is an instructive limiting case. Q_o was set equal to 2.2.

Figure 1 summarizes the computational results for monodisperse aerosols. The figure shows the accuracy of the technique and presents the ratio of the predicted Scatometer volume using Equation (10) to the true aerosol volume versus diameter (or size ratio, r/λ), refractive index, and forward scattering angle. The points are the midpoints of the size distributions defined in Equation (11). A perfect response would be represented by a horizontal line. For diameters greater than about 5 μm, the effect of refractive index becomes unimportant for angles of 0, 1/2, and 1 degrees.

The solid line is a transmissometer response (extinction cross section per unit volume of aerosol) for a refractive index of 1.5 and is normalized to the same peak height as the Scatometer for comparison. The severe loss of response for large particles is typical and results as extinction becomes proportional to particle cross section, not volume, for diameters greater than approximately 2 μm. Note the improved response the Scatometer offers for larger particles. For nonabsorptive small aerosols, the Scatometer is about equivalent to the transmissometer. For absorptive materials, such as carbon, transmissometer response is much worse, reaching a peak of 5.6 at 0.23 μm while following the flyash curve for particles greater than 2 μm.

The horizontal axis of the graph in Figure 1 is particle diameter, however, the response depends only on the ratio of particle size to wavelength and this axis could be labeled as the ratio r/λ. For the wavelength of 1/2 μm, r/λ is equal to d, and the scales are identical. A change in wavelength would simply change the diameters in direct proportion without changing the shape of the response curve. Thus, response for a wavelength of 1 μm is identical to that shown in Figure 1 except that the diameters would be doubled.

The data in Figure 1 show that of the refractive indices analyzed, soot can be measured with greatest accuracy. For particles larger than 2 μm in diameter the technique works well for all materials examined and the response closely resembles that predicted from the diffraction and extinction approximation, Equations (2) and (6). The cyclic response variations in the range $1 \leq d \leq 3$ will be averaged out by any size distribution encountered in the field. For $d < 1$, response is highly dependent on both size and refractive index. As the real part of the

refractive index increases, the response increases and the peak moves to smaller sizes. This trend is also apparent in Figure 2. Increasing absorption smooths the curve and extends the small size sensitivity; this effect can be seen for both the absorptive fly ash and carbon curves. For the refractive indices tested, the high response peak results primarily from a large increase, approximately a factor of 4, in the forward scattering over that predicted by the diffraction approximation. The increase in the extinction cross section over Equation (6) is not nearly as great, approximately a factor of 2.

For particles smaller than 0.5 μm the Scatometer response drops off rapidly, primarily due to the sudden decrease in forward scattering (much more rapidly than r^4 as given by Equations (2) and (3)). The extinction cross section of non absorptive materials also diminishes rapidly (as r^3 with respect to particle volume). For absorptive materials, the extinction cross section with respect to volume becomes a constant depending only on the imaginary part of the refractive index. For carbon and absorptive flyash these cross sections are about 40 percent and 4 percent of their peak values respectively. This limited cross section decrease extends the response to smaller particles.

The response variation between 0.3 and 5 μm is a result of Mie scattering effects; the diffraction and extinction approximations used (Equations (1) and (6)) predict a flat response below 5 μm.

Figure 2 illustrates the predicted response variation for small changes in refractive index (m = 1.45, 1.5, and 1.55). For m = 1.6, not shown, the maximum response is 2.98 at 0.49 μm. The other ranges of refractive indices in Group 2, Table 1, show less variation in response and the calculations confirm the insensitivity of the Scatometer technique response to changes in refractive index. Again, the response trend as the real part of the refractive index increases is evident: the peak gradually increases in height and moves to smaller sizes.

Figure 3 specifically illustrates response at forward scattering angles up to 10° (m = 1.5 in this case). The response is nearly identical for all indices tested. This independence is expected because diffraction which is independent of refractive index is the major factor. As can be seen, and as indicated by Equation (1), large particle response decreases rapidly with increasing size and scattering angle. The results indicate that the upper size limit is nearly inversely proportional to the scattering angle, again as expected from Equation (1). The data for $\theta = 0$ indicate the high accuracy of the technique for small scattering angles and large particle diameters.

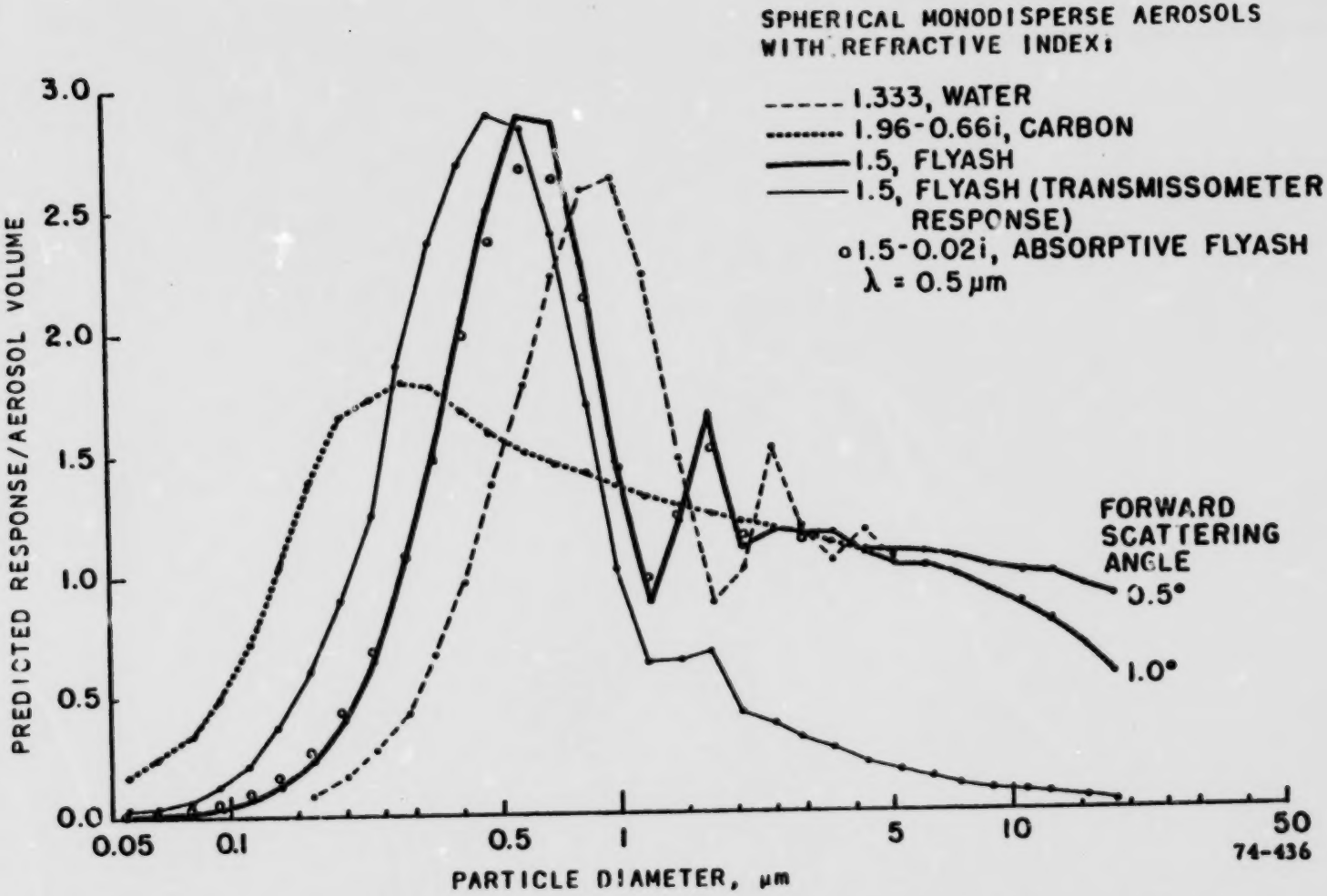

Figure 1. Predicted Scatometer response per unit volume of typical aerosols as a function of particle size

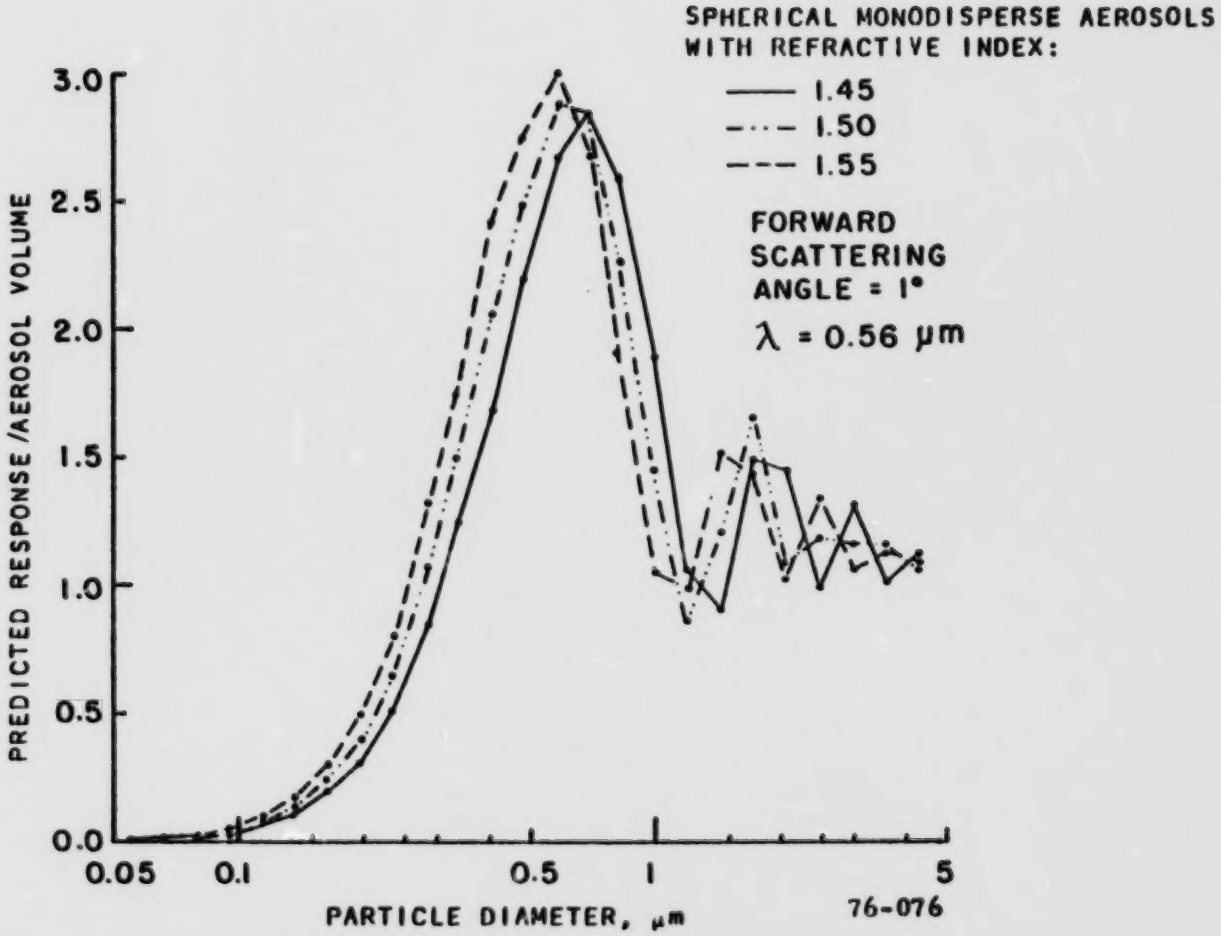

Figure 2. Predicted Scatometer response per unit volume of aerosol as a function of particle size and changes in refractive index

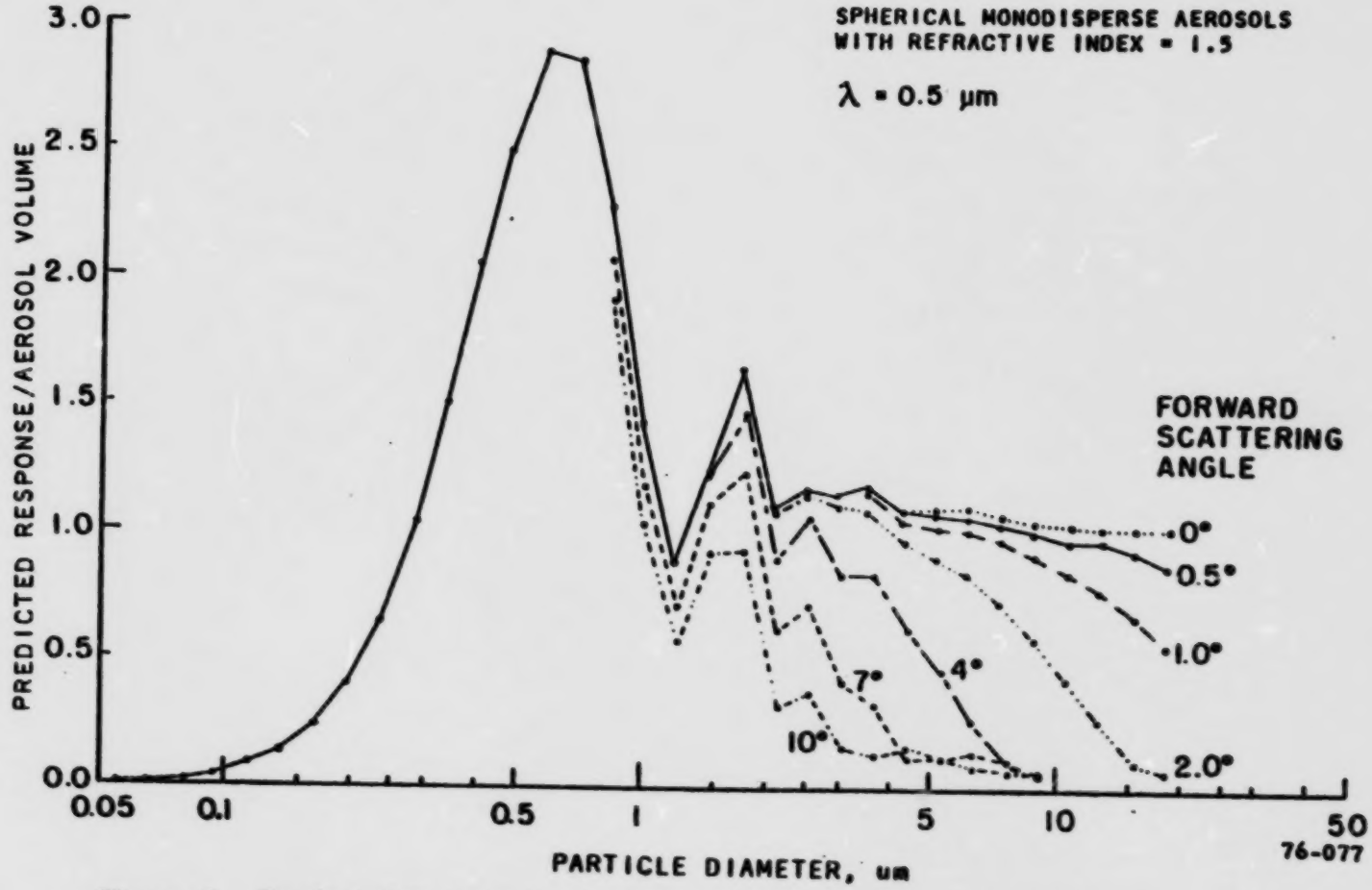

Figure 3. Predicted Scatometer response per unit volume of aerosol as a function of particle size and various scattering angles

The calculations for monodisperse aerosols indicate that the Scatometer technique performs well over a broad size range and is insensitive to change in refractive index. The results also form a good basis for comparing theory with experimental measurements.

Polydisperse Aerosol Calculations

Monodisperse aerosols are not normally found in industrial emission sources, and the monodisperse results presented above must be averaged over practical size distributions in order to obtain a realistic prediction of response in real environments. It is important to note that the polydisperse aerosol response will be an improvement over monodisperse aerosol results because the fluctuations will be averaged out. Averaging will include the error introduced through the approximation given by Equation (8). This error is negligible for the monodisperse size distributions used earlier and becomes significant only for wide size distributions. Most size distributions encountered in the field will, in addition, include particles outside of the response range of the Scatometer and it is important to investigate the effect of this limited range on overall accuracy.

Lognormal size distributions, Equation (13), with respect to volume were selected to model the distributions likely to be encountered in the field:

$$\frac{dV}{d\,(\ln d)} = N_o \exp\left[\frac{-(\ln d - \ln d_g)^2}{2 \ln^2 \sigma_g}\right] \qquad (13)$$

where d_g specifies the median volume diameter (geometric mean diameter) and σ_g the polydispersity, i.e., the geometric standard deviation.

N_o is chosen so that

$$N_o \int_{-\infty}^{+\infty} \frac{dV}{d\,(\ln d)}\, d\,(\ln d) = 1.$$

This form of size distribution was selected because it appears to fit typical mass distributions measured in the field. The Scatometer

response was determined by averaging the monodisperse forward scattering and extinction cross sections over the size distribution as shown below:

$$\sigma(d_g, \sigma_g, \theta) = \int_{-\infty}^{+\infty} \sigma_p(d, \theta) \frac{dV}{d \ln d} \, d \ln d \tag{14}$$

$$\sigma_e(d_g, \sigma_g) = \int_{-\infty}^{+\infty} \sigma_e(d) \frac{dV}{d \ln d} \, d \ln d \tag{15}$$

and then calculating Scatometer response from Equation (10) using these averaged cross sections. A wide range of d_g and σ_g were used to include any size distribution likely to be encountered in the field.

The integrals of Equation (14) and (15) are time consuming to evaluate, particularly if $\sigma_p(d, \theta)$ and σ_e must be recalculated each time d_g or σ_g is changed; thus, for purposes of calculation these integrals were converted to the following sums (note that $d_g/2 = r_g$):

$$\sigma(r_g, \sigma_g, \theta) = \ln \frac{r_{max}}{r_{min}} \sum_{1}^{n} \overline{\sigma(r_i, \theta)} \frac{dV(r_i)}{d \ln r_i} \tag{16}$$

$$\sigma_e(r_g, \sigma_g, \theta) = \ln \frac{r_{max}}{r_{min}} \sum_{1}^{n} \overline{\sigma_e(r_i)} \frac{dV(r_i)}{d \quad r_i} \tag{17}$$

$\overline{\sigma(r_i, \theta)}$ and $\overline{\sigma_e(r_i)}$ are similar to the averaged cross sections used for monodisperse calculations except that narrow constant volume size distributions, $\eta_i(r)$, were used instead of distributions uniform with respect to number as in Equations (11) and (12). Mathematically, these distributions are defined as

$$\eta_i(r) = A/r^3, \; r_{min_i} \leq r \leq r_{max_i}$$

$$\eta_i(r) = 0 \quad \text{Otherwise} \tag{18}$$

and $$r_{max_i}/r_{min_i} = 1.2$$

A is chosen such that

$$\int_0^\infty \eta_i(r)\,(4/3)\,\pi\,r^3\,dr = 1 \tag{19}$$

The averaged cross sections are more precisely:

$$\overline{\sigma(r_i, \theta)} = \int_{r_{min_i}}^{r_{max_i}} \sigma(r, \theta, m)\,\eta_i(r)\,dr \tag{20}$$

$$\overline{\sigma_e(r_i)} = \int_{r_{min_i}}^{r_{max_i}} \sigma_e(r, m)\,\eta_i(r)\,dr \tag{21}$$

Each r_i is the midpoint of r_{min} and r_{max}; and $r_{i+1} = 1.2\,r_i$. The averaged cross sections were calculated using the same program used to calculate the monodisperse results with only a small change in a subroutine. This output was then input to a separate program which evaluated Equations (16) and (17). The advantages to this approach are that recalculation of the Mie cross sections are avoided for different size distributions and that the necessary scattering information is contained in a relatively small array of numbers. The sums, in Equations (16) and (17), need be only over the sizes which contribute significantly to the cross sections. Equation (6) may be used to calculate extinction cross sections for large diameters. Once Equations (20) and (21) are evaluated the computer cost for calculating response to any lognormal size distribution is approximately one cent each. For accuracy of a few percent, σ_g, must be larger than 1.4.

Figures 4 through 7 illustrate calculated Scatometer and transmissometer response for the polydisperse lognormal size distributions described above; the response is much flatter than for monodisperse aerosols. A wavelength of 0.56 μm was used to allow direct comparison with experimental work in which a photopic filter was used. The results can be simply converted to other wavelengths, λ_a, by multiplying the x axis scale by $\lambda_a/0.56$.

Figure 4 shows Scatometer relative response for fly ash (m = 1.5) at a scattering angle of 1/2°, median volume diameters from 0.1 to 20 μm, and geometric standard deviations from 2 to 8. The response is accurate to about ± 30 percent for sizes from 0.3 to 20 μm and geometric standard

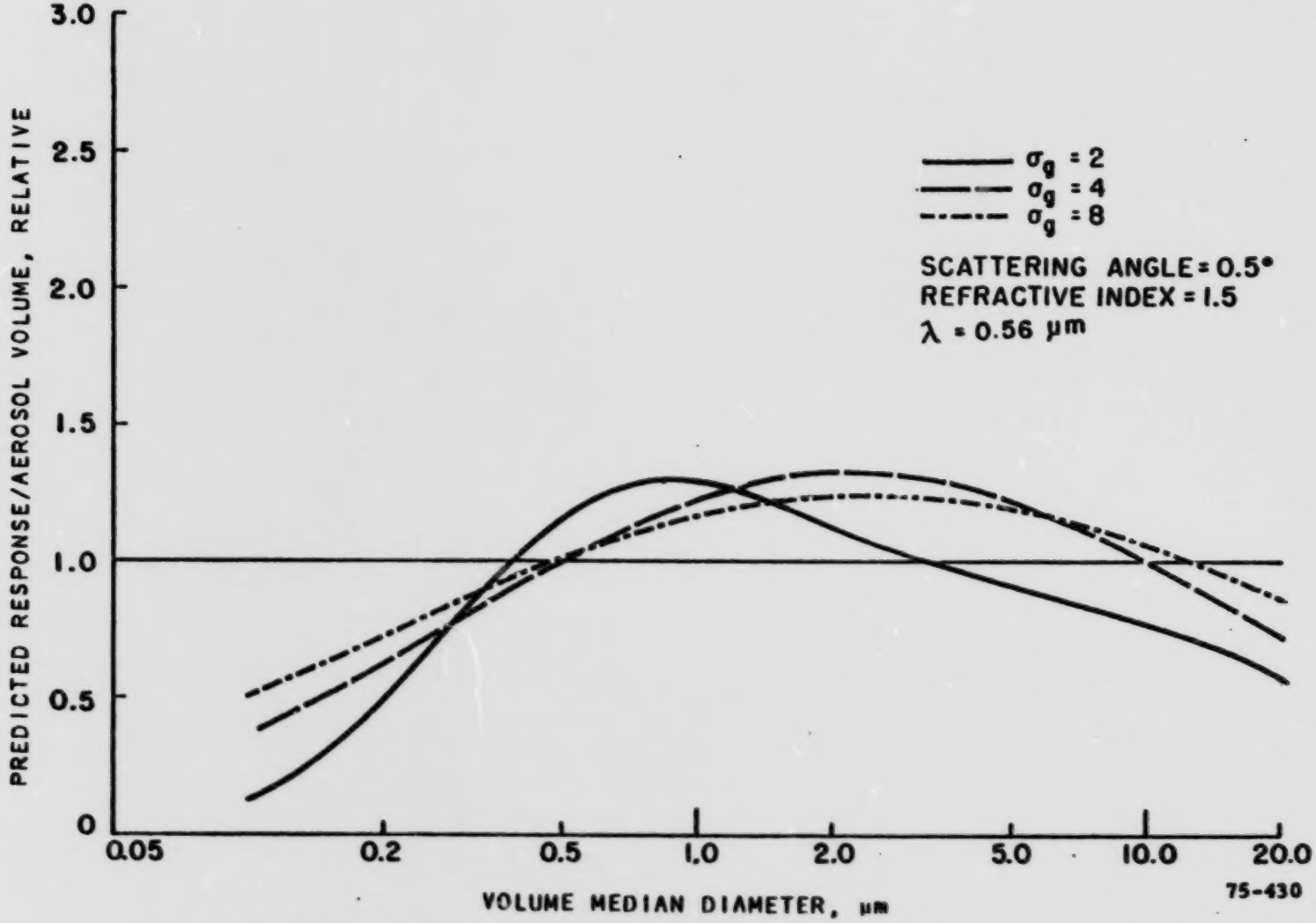

Figure 4. Predicted Scatometer response per unit volume of aerosol as a function of the size parameters of lognormal volume distributions, θ = 0.5°

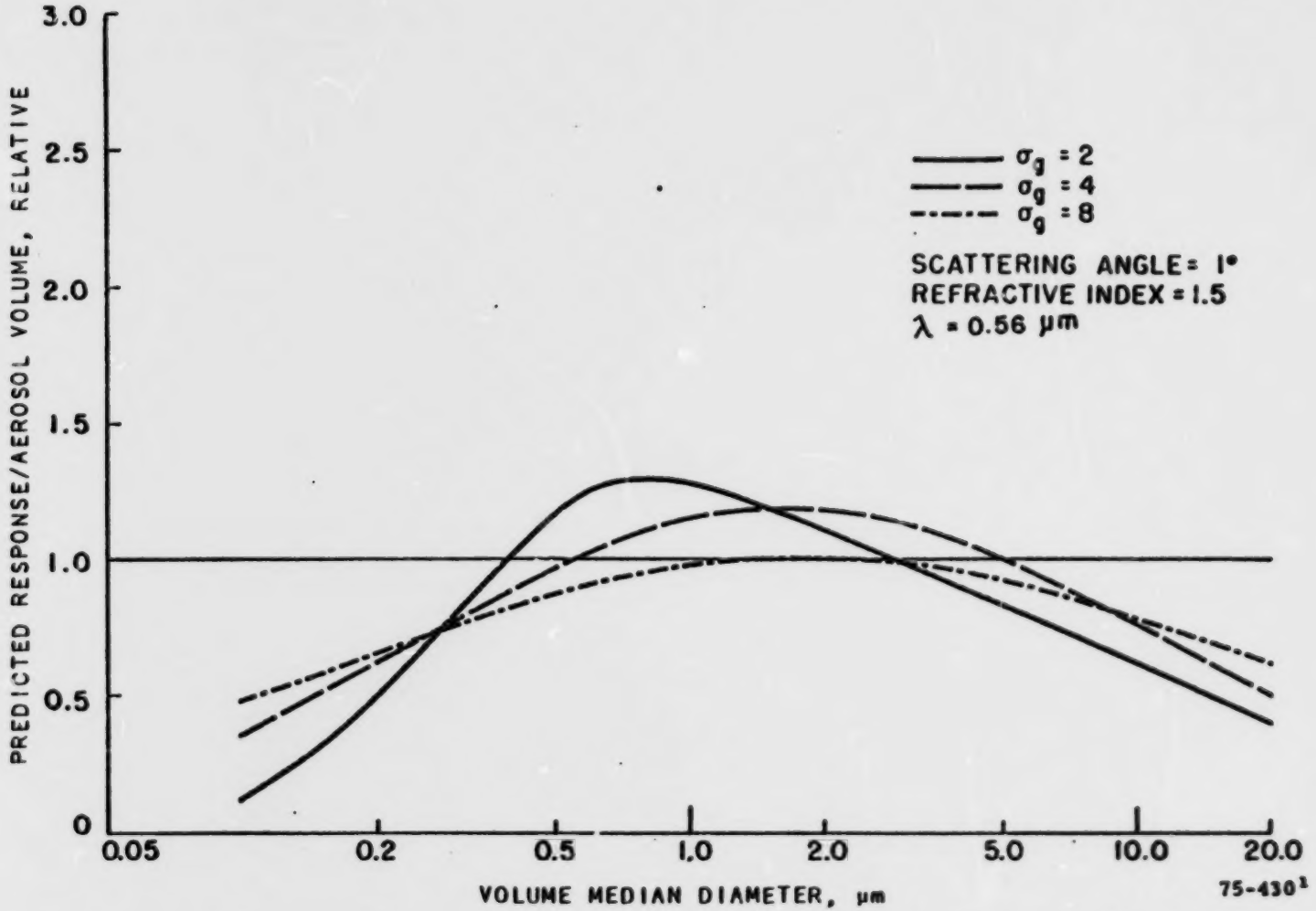

Figure 5. Predicted Scatometer response per unit volume of aerosol as a function of the size parameters of lognormal volume distributions, θ = 1°

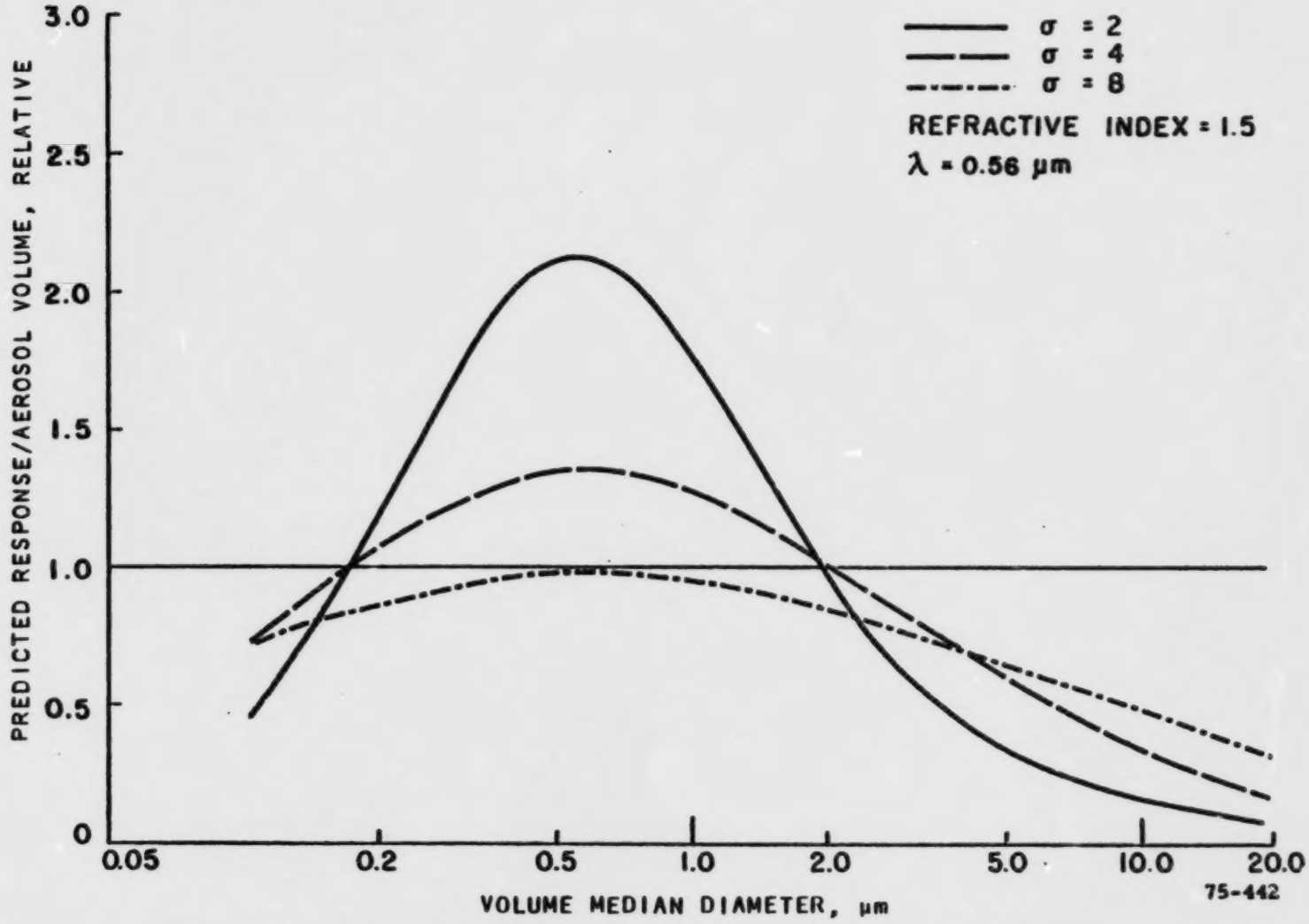

Figure 6. Predicted transmissometer response per unit volume of aerosol as a function of the size parameters of lognormal volume distributions

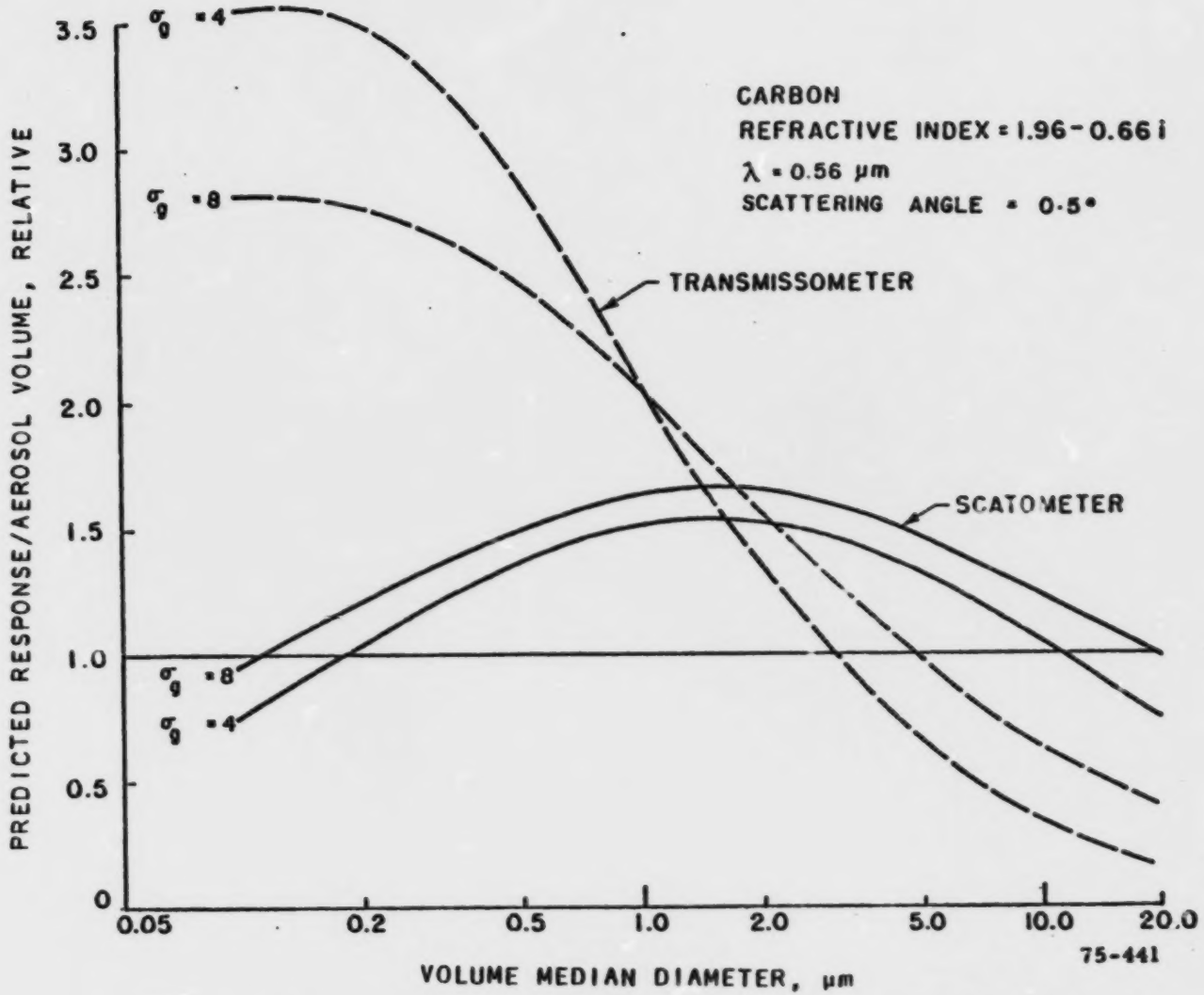

Figure 7. Comparison of predicted Scatometer and transmissometer response per unit volume of aerosol as a function of the size parameters of lognormal volume distributions for carbon

deviations from 4 to 8, the ranges of parameters likely to be encountered in a typical stack. Note the independence with respect to polydispersity. Over smaller size ranges, the technique is more accurate. In actual use, the results will be correlated to mass by a number of mass determinations to convert the volume measurement to mass. This procedure will have the effect of multiplying all points on the graph by a constant and in this way the accuracy can be optimized over a particular size range if desired.

The vertical axis of Figure 4 has been labeled "relative response" (Figures 1-3 are absolute response) because the points plotted are the absolute response divided by 1.5. This systematic difference stems from two factors: (1) the Equation (8) approximation, for $\overline{r^3}$, $(\overline{r^2}\,\overline{r^4})^{\frac{1}{2}}$, is greater than $\overline{r^3}$ for polydisperse size distributions, and (2) the average Scatometer response for particles from 0.5 to 15 μm diameter is approximately 1.4. As the polydisperity increases the error in Equation (8) tends to offset the response loss from particles outside the response range.

Figure 5 illustrates Scatometer relative response (absolute response divided by 1.5) for the same parameters as Figure 4 except for a forward scattering angle of 1°. Notice that the response is very similar to that at 1/2°, Figure 4. This result is important because a 1° instrument is easier to construct than a 1/2° instrument. For mean diameters less than approximately 5 μm, the response is flatter than for 1/2°; however, the response is somewhat more sensitive to changes in polydispersity. As expected, response decreases more rapidly for particles larger than 5 μm but not as quickly as might be expected from the monodisperse aerosol results.

Figure 6 shows predicted transmissometer response (aerosol volume equal to the extinction coefficient or cross section multiplied by a constant) for the same aerosols used in Figures 4 and 5. The constant of proportionality, i.e., the normalization constant, has been chosen so the peak of the response curve for $\sigma_g = 4$ is the same height as the Scatometer response curve for $\sigma_g = 4$. This choice allows the response flatness to be easily compared. Note the sensitivity of the transmissometer to polydispersity for particles less than 2 μm diameter. For polydisperse aerosols between 0.2 and 2 μm, the transmissometer is slightly less sensitive to changes in size than the Scatometer and could be used on sources where the aerosol size is within this range and the polydispersity is relatively constant.

Figure 7 compares predicted relative Scatometer and transmissometer response to a carbon aerosol, such as might be expected when blowing soot. The peak Scatometer response for carbon particles with $\sigma_g = 4$ is 14 percent higher than for flyash. For particles with $\sigma_g = 8$ it is 23 percent higher. (The peak for $\sigma_g = 2$, not shown is 9 percent lower.) The small particle response is extended in all cases. The sensitivity to

refractive index change is much less than that of the transmissometer whose small particle response changes dramatically with a change in refractive index. The increase in Scatometer peak height is primarily due to the error introduced by the approximation given in Equation (8).

Results for other polydispersities σ_g = 1.5, 3, 6, and 10, and other refractive indices have also been calculated. Figures 4 through 7 have been selected to illustrate the major features of the theoretical Scatometer response.

CORRECTION TECHNIQUES

Error in the Scatometer algorithm can be significantly reduced by several methods. These techniques generally work extremely well over a small range of parameters and moderately well over extended ranges. Their sensitivity to changes in refractive index needs further investigation.

One technique uses the ratio of the forward scattering to extinction cross section to deduce a correction factor for basic Scatometer response, Equation (10). The corrected response (from Figure 4) is shown in Figure 8. As can be seen, the correction is perfect for σ_g = 4. For polydispersities likely to be encountered in the field, i.e., $\sigma_g \geq 4$, the response becomes almost independent of particle size. The correction is made by computing the forward scattering to extinction ratio vs size for a selected σ_g (4 in the case of Figure 8) and then matching that ratio with a multiplicative correction factor equal to the reciprocal of the Scatometer response. Since scattering ratio increases monotomically with respect to size, the correction factor is unique. The basic Scatometer response for an arbitrary aerosol is corrected by (1) calculating or measuring the forward scattering to extinction ratio, and (2) multiplying the correction factor determined from the selected polydispersity times the uncorrected response. If the polydispersity is different, some additional error will be introduced as in Figure 8. A second difficulty with this ratio method is that it is not as independent of refractive index as the basic Scatometer technique, Equation (10). Further work is likely to reduce this dependency.

It is possible to improve the correction by limiting the range over which it is used. For example, size distributions with median diameters less than 0.2 μm (or σ_g<3) are not likely to be encountered and the correction can be improved above 0.2 μm diameter by sacrificing accuracy below that size. This improvement looks promising and further evaluation is desirable.

Other correction methods exist which employ scattering at more than one angle. It appears possible using scattering at two angles and extinction to correction Equation (10) for an arbitrary lognormal size distribution.

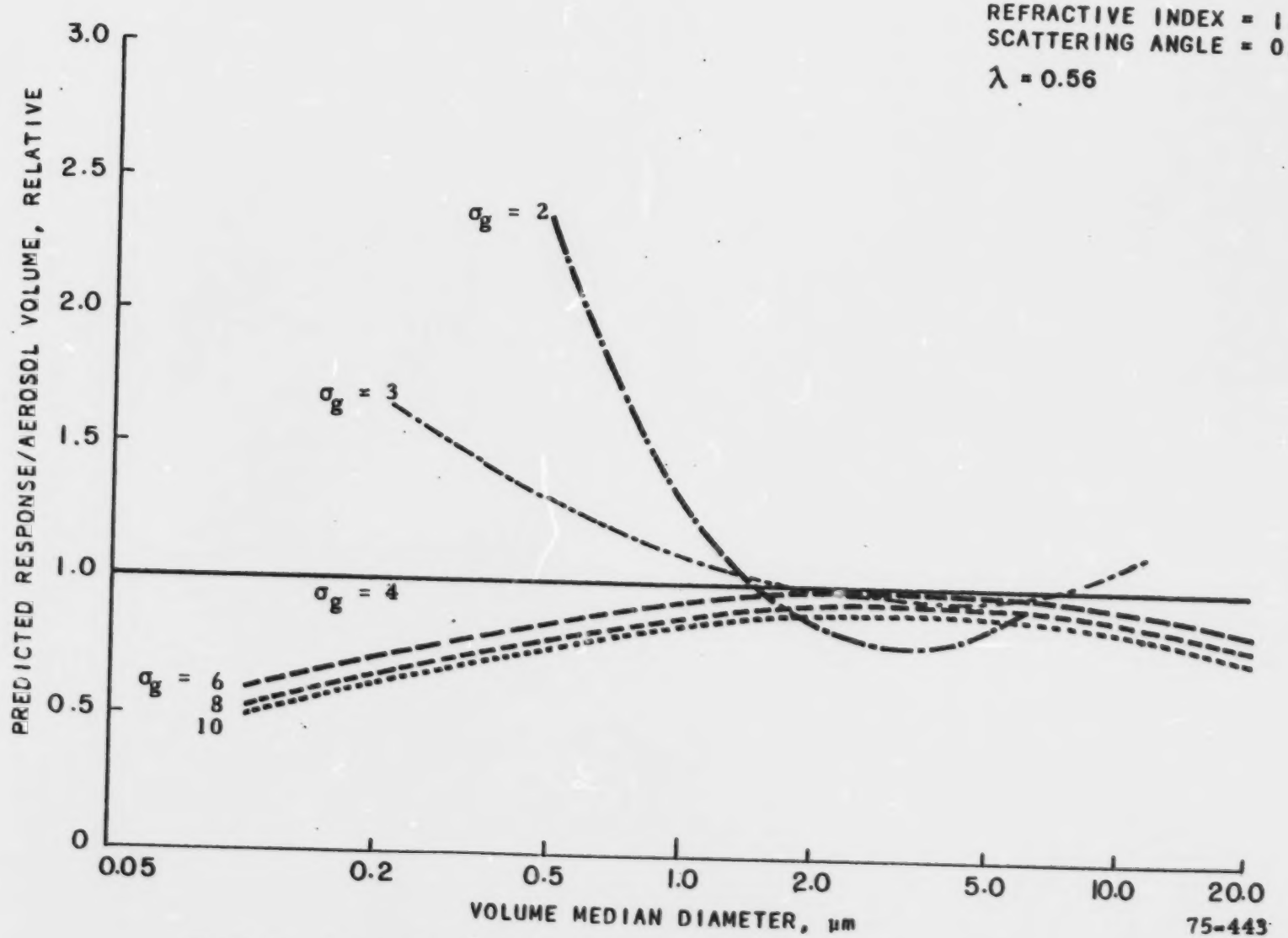

Figure 8. Corrected Scatometer response per unit volume of aerosol as a function of the size parameters of log normal volume distributions

In addition, this method will provide more information about the size distribution, i.e., both d_g and σ_g will be determined. This method, therefore, looks exceptionally promising. Sensitivity to refractive index has not yet been determined. If scattering at multiple angles is measured, it becomes possible to determine a number of parameters of the size distribution.

ACTIVE VOLUME CONSIDERATIONS

Calculations to determine the active volume of the Scatometer chamber have been performed. Due to the Scatometer geometry, not all light scattered by the aerosol in the chamber at a given angle is received by the detector, see Figure 9. The volume from which scattered light is collected is referred to as the active volume, V_A, and its ratio to the total volume of the light beam in the chamber is the active volume ratio. For small angles the ratio is nearly 1; for large angles, only a fraction of the volume is active. The active volume ratios are needed to properly weight the scattering intensities seen by the detector at different angles. The active volume ratio, $R(\theta)$, depends on the following dimensions:

θ = the scattering angle

R_L = lens radius

R_B = beam radius

D = length of aerosol chamber

D_S = distance from aerosol chamber to lens

The total active volume is calculated by integrating the active cross section over the length of the chamber:

$$V_A = \int_{D_S}^{D_S + D} A(x)\, dx \qquad (22)$$

where $A(x)$ is the active cross section at position x. A typical cross section is shown in Figure 9. The active cross section is defined by the intersecting segments of two circles, i.e., the projection of the scattered light beam at a given scattering angle onto the focusing lens. The active area is given by the following expressions:

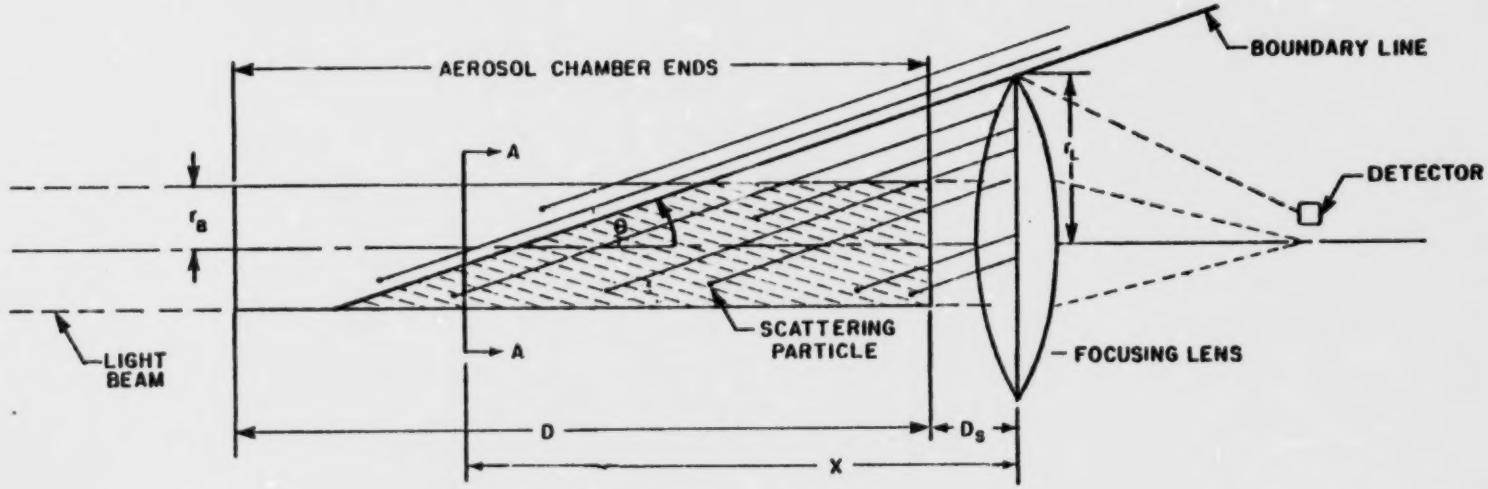

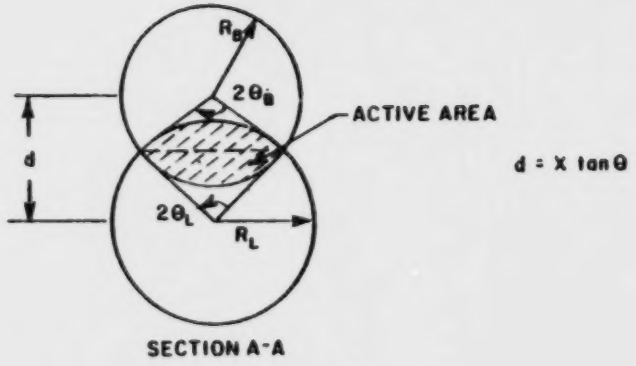

Figure 9. Active scattering volume (shown hatched)

$$A(X) = \frac{1}{2} R_L^2 (2\theta_L - \sin 2\theta_L) + \frac{1}{2} R_B^2 (2\theta_B - \sin 2\theta_B) \quad (23)$$

$$\theta_L = \cos^{-1}\left(\frac{R_L^2 - R_B^2 + d^2}{2 R_L d}\right), \quad \theta_B = \cos^{-1}\left(\frac{R_B^2 - R_L^2 + d^2}{2 R_B d}\right) \quad (24)$$

$$d = X \tan\theta$$

Because of the complexity of the above equations, the integral in Equation (22) was evaluated numerically; a FORTRAN program was written for this purpose. The program computes the active volume, V_A, and $R(\theta)$, the ratio of the active volume to the full beam volume in the aerosol chamber, $\pi R_B^2 D$.

Table 2 shows results for two typical cases, one using a 3.8 cm radius lens (3 inch diameter) and the other using a 7.2 cm radius lens (6 inch diameter). The aerosol chamber length is 122 cm, the beam diameter 2.54 cm, and the separation distance 10 cm. As can be seen, the 6 inch lens allows intensity measurements to about twice the angle of the 3 inch lens. The computer program permits quick and easy calculation of weighting factors as the dimensions are adjusted in the experimentation process.

Table 3 indicates the active volume ratios for the Scatometer geometry and scattering angles used in the experimental work.

TABLE 2

Active Volume and Active Volume Ratios

	Lens Radius, R_L			
	3.8 cm		7.6 cm	
Scattering Angle θ	Active Volume V_A	Active/Total Volume $R(\theta)$	Active Volume V_A	Active/Total Volume $R(\theta)$
1.0	2.4 liters	0.96	2.5 liters	1.00
2.0	1.8	0.72	2.5	1.00
3.0	1.2	0.48	2.4	0.96
4.0	0.84	0.34	2.0	0.79
5.0	0.62	0.25	1.5	0.62
6.0	0.49	0.20	1.2	0.51
7.0	0.39	0.16	1.0	0.42
8.0	0.31	0.13	0.88	0.36
9.0	0.26	0.11	0.77	0.31
10.0	0.21	0.09	0.67	0.27

Beam Radius, R_B = 2.54 cm

Test Chamber Length, D = 122 cm

Distance of Focusing Lens from Chamber, D_S = 10 cm

TABLE 3

ACTIVE VOLUME RATIOS FOR CURRENT SCATOMETER GEOMETRY

Beam Radius, R_B	=	2.65 cm
Lens Radius, R_L	=	5.1 cm
Chamber Length, D	=	180.0 cm
Distance from Chamber to Lens, D_S	=	2.0 cm

Angle	1/2°	3/4°	1°	1-1/2°	2°	2-1/2°	3°
Active Volume Ratio	1.00	1.00	0.99	0.90	0.76	0.62	0.51

SECTION 5

EXPERIMENTAL STUDIES

EXPERIMENTAL DESIGN

The experimental program provided (1) feasibility demonstrations of the Scatometer technique and (2) error evaluations using controlled laboratory aerosols. Aerosol particles ranged from 0.5 to 6 μm diameter. Monodisperse aerosols were used where possible to allow simple interpretation of results and clear comparisons with theory. Polydisperse aerosols were also included to simulate real stack aerosols. Although size distribution measurements are more difficult for the polydisperse aerosols, experimental results compared well with theoretical predictions.

Initial Experimental Apparatus

A diagram of the initial experimental design is shown in Figure 10. The collimating and focusing lenses are camera elements approximately 25 mm (1 inch) in diameter and focal lengths of 55 and 135 mm, respectively. The detectors are located in the focal plane of the focusing lens. All light scattered at a given angle, θ, is focused into a ring on the focal plane. The radius, $r_s(\theta)$, is given by

$$r_s(\theta) = r_f \tan \theta \tag{25}$$

where r_f is the focal length and θ the scattering angle. By traversing the scattering detector radially from the optical axis, the scattered intensity at different angles is measured. For typical aerosols the scattered light forms an image in the focal plane that appears as a high intensity point of light surrounded by a dim halo (about 10^{-5} as bright) whose intensity diminishes with increasing radius.

Figures 11 and 12 show initial results using photograph film in the focal plane. The bright center and halo are evident. Scattering was produced by a "simulated aerosol" consisting of 0.5 μm diameter latex spheres deposited on a glass plate located 7 cm in front of the lens. Light scattered at 1° lies 1.9 cm from the center. The pictures confirmed the anticipated intensity variation of the scattering pattern.

The initial experiments also used a light pipe with a small aperture on one end to scan the scattered light image. The output was interfaced into a simple photodetector to provide quantitative measurements.

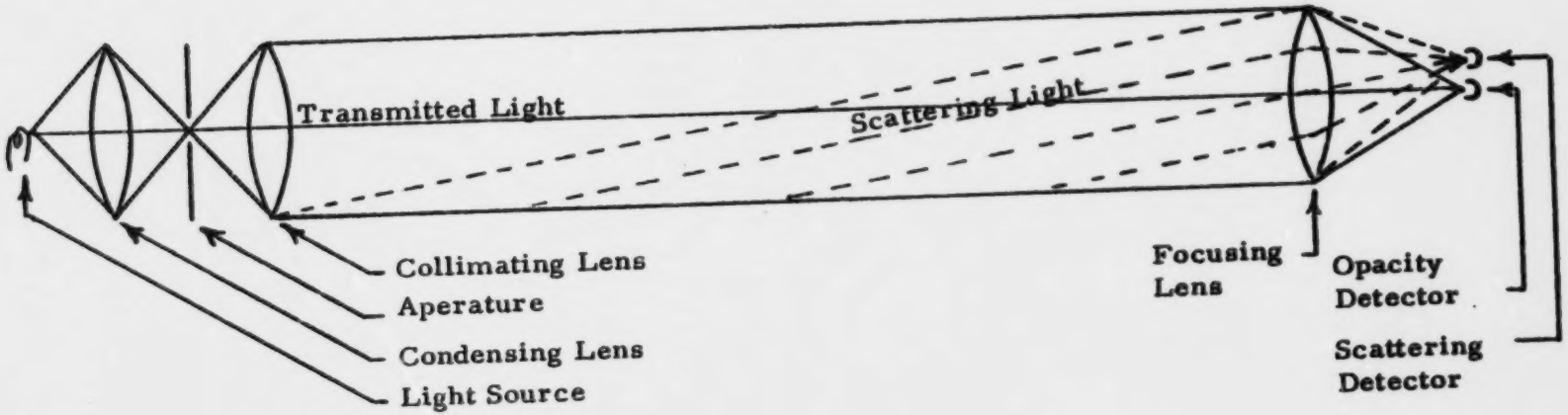

Figure 10. Diagram of optical arrangement for initial scattering-opacity experiments

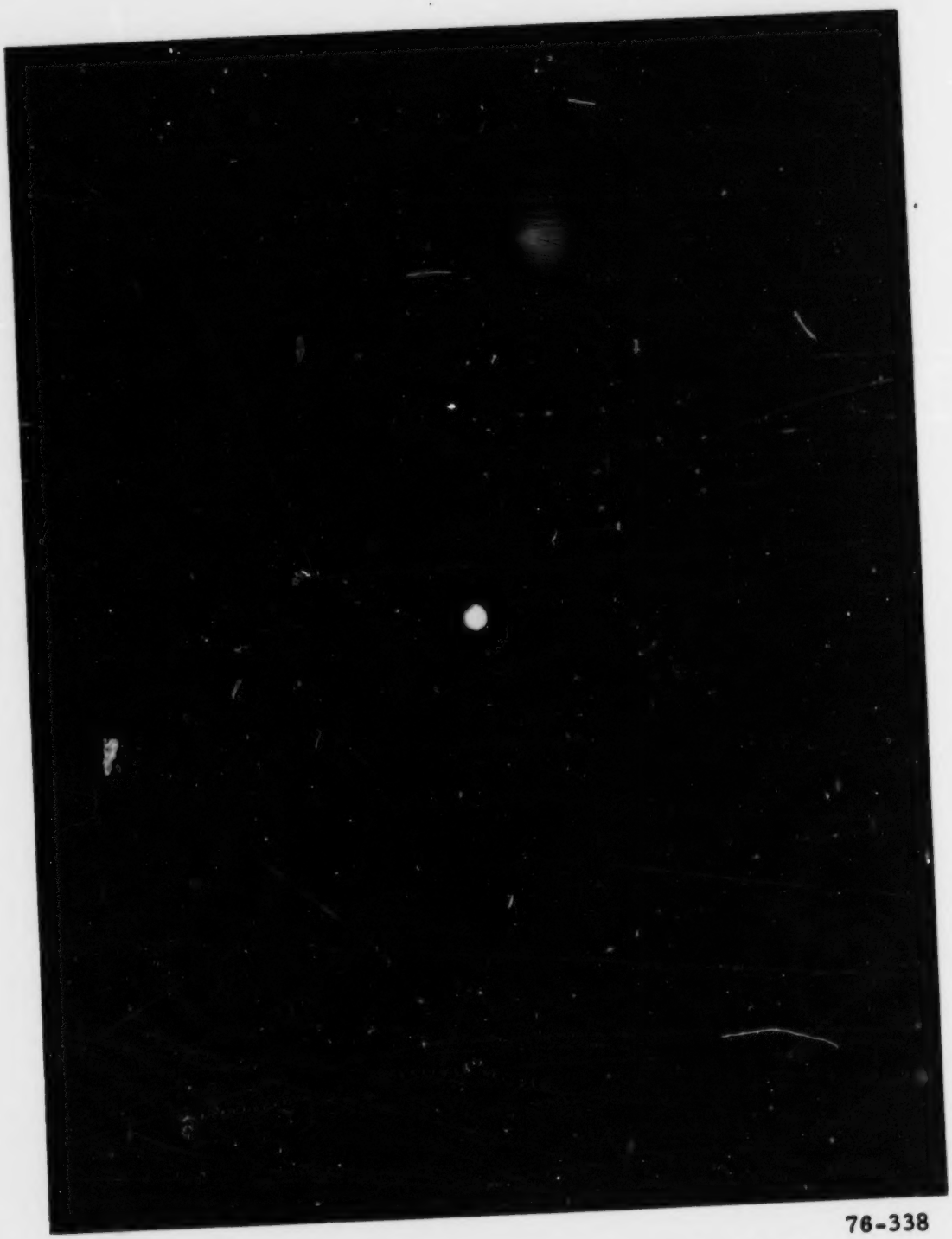

76-338

Figure 11. Light image in the Scatometer focal plane with no aerosol present

76-339

Figure 12. Light image in the Scatometer focal plane with a simulated aerosol in the beam

The initial apparatus indicated qualitative agreement with expected performance and also uncovered several difficulties.

The active volume calculations indicated that the focusing lens diameter was insufficient to collect light scattered at angles greater than 1° beyond 0.6 meters from the lens. For sufficient opacity, 10 to 20 percent, a chamber at least 1.8 meters long was needed.

The original small lenses were replaced by large aerial camera lenses. The focusing lens was 19 mm (4 in.) diameter with a focal length of 61 cm (24 in.). The large lens collected scattered light to about 3°, as shown by the active volume calculations, Table 3. The 61 cm (24 in.) focal length of the final lens produced an image large enough to work with easily. The larger lenses, however, contained imperfections that caused high background scattering even with no aerosol in the chamber. This scattering varied greatly between $1/2^{\circ}$ and 3°. To make measurements at multiple angles the detector needed to be repositioned very carefully so that the background (typically 4 to 15 times larger than the aerosol scattering) could be accurately subtracted out. This problem was solved by mounting the detector on a milling machine cross-feed table.

One of the most serious difficulties encountered during the initial work was the relatively low intensity of the scattered light. The first detector system using a light pipe arrangement did not have sufficient range to measure both the scattered light intensity and the power in the transmitted beam. Typically, this ratio was 10^{-8}. Measurement of this ratio is critical in determining the scattering cross section.

The problem was solved by using an improved photometer, a United Detector Technology 80-X, with a dynamic range of 10^{+8}, from 10^{-4} to 10^{4} microwatts/cm^{2}. The photometer detector was fitted with an aperture and positioned in the focal plane. This design eliminated the light pipe and its losses.

Finally, a much more rigid and convenient optical bench was constructed. The new bench greatly reduced alignment and vibration problems.

Aerosol Generation

In order to experimentally evaluate performance of the Scatometer, it was necessary to generate controlled reproducible test aerosols. It was also necessary to know the physical properties and concentration of these aerosols. Typically an extinction coefficient of 0.05 per meter was needed for sufficient opacity in the 1.8 meter scattering chamber. Monodisperse aerosols were produced by nebulization of a water suspension of uniform polystyrene latex spheres. (These suspensions, 10 percent

spheres by volume, are commercially available in a wide range of sizes from Dow Chemical Company, Midland, Michigan.) The nebulized water drops evaporate leaving an aerosol of spherical particles with known composition, refractive index, and particle size. If the suspension has been sufficiently diluted, each droplet will contain at most one sphere and the resulting aerosol will be monodisperse without agglomerates. This method of aerosol generation is discussed more fully and the necessary dilution ratios are calculated by Raabe.[8]

A diagram of the MRI Aerosol Generator is shown in Figure 13. Originally, an ultrasonic nebulizer was installed for producing spray droplets because it was more convenient than the sprayer shown in the drawing. These devices produce droplets in the 0.1 μm diameter size range which then coalesce to produce the 2-8 μm drops observed in its output. Because the original droplets are smaller than the suspended spheres, no spheres appeared in the nebulizer output. The ultrasonic nebulizer was replaced with a spray nozzle and baffles were added to impact out the larger water droplets that contained more than one latex sphere. This design was useful in producing relatively monodisperse aerosols of 2 μm diameter spheres; it unfortunately consumed large quantities (20 ml per minute) of suspension, and lacked stability. It was also not usable for 6 μm spheres.

These problems were solved by using two Collison (BGI) and two Retec X-70/N nebulizers [9,10]. Their outputs were much more stable and latex suspension consumption rates much lower. The Collison nebulizers were used to produce 2 and 0.5 μm PSL and PVL (polystyrene and polyvinyl toluene latex) aerosols. The larger drop size produced by the X-70/N, 2-10 μm, was needed to generate the 6 μm PSL aerosol.

Revised Scatometer Design

The current Scatometer design is diagramed in Figure 14 and pictured in Figures 15-17. The design is similar to the initial design shown in Figure 10 but with an improved light source, detector system, lenses, and optical bench. The basic optical design is unchanged. A collimated light beam is projected through the aerosol chamber. The beam and forward scattered light are collected by the focusing lens and imaged at its focal plane. A movable detector is used to measure the transmitted beam power and scattered light intensity. A separate detector is used to monitor fluctuations in the original beam intensity. The overall length of the system is 4.8 meters.

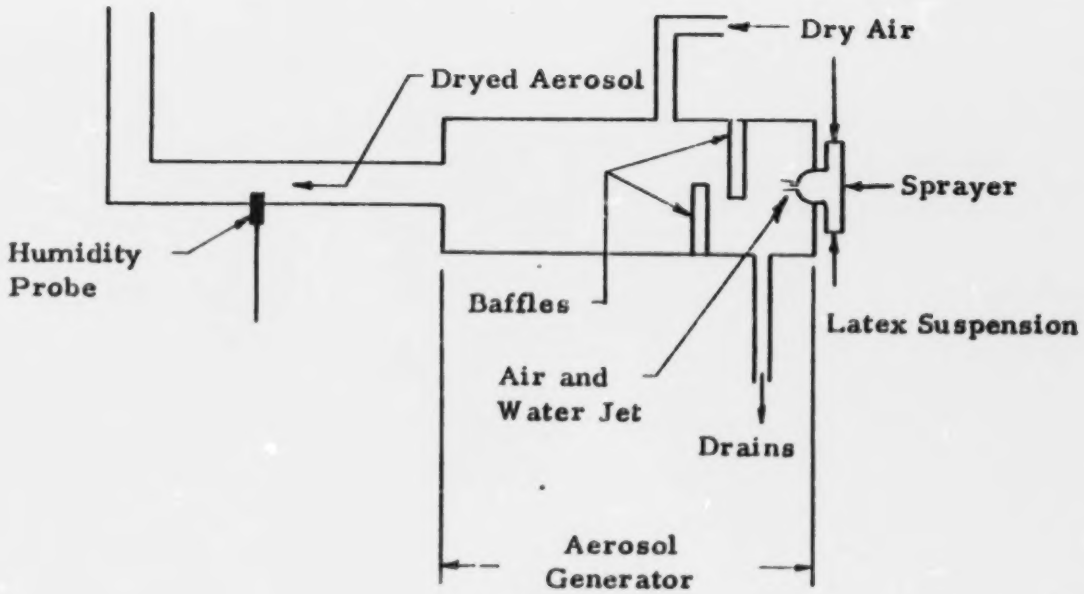

Fig. 13. Diagram of aerosol generator

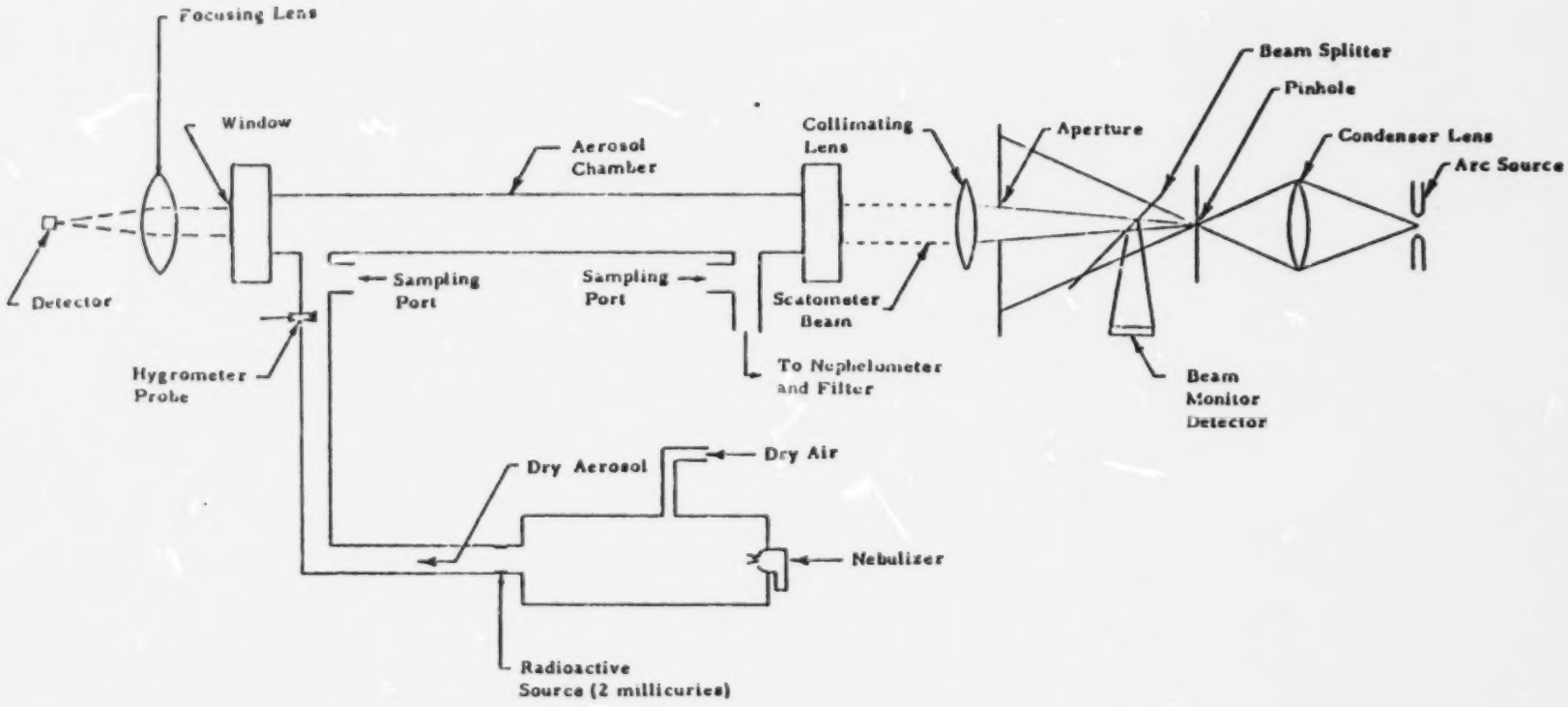

Figure 14. Scatometer diagram

Figure 15 shows the basic Scatometer experimental configuration. The optical bench is constructed from two aluminum I beams, and supported by two machine shop benches. The collimating f3.5 lens has a focal length of 356 mm (14 in.). The aerosol chamber is 180 cm in length. The window is visible on the forward end. The photometer is used to monitor the optical beam intensity. The focusing lens has a focal length of 607 mm (24 in.) and an f 6 aperture. The detector stage includes a traversing mechanism and the detector of a second photometer. A photopic filter is included in the detector housing to limit the detector to the standard photopic response.

Figure 16 is a close-up of the traversing mechanism and detector. The traversing mechanism is constructed out of two standard milling tables and allows repeatable positioning of the detector to 0.025 mm (0.001 in.). The entire assembly slides along the optical bench rails for detector positioning in the third dimension. The black cylinder fastened by a hose clamp near the center of the picture is the detector housing. The detector aperture is visible in the center of the black disc fastened to the front end. The detector angle of view is 0.19 degrees.

Figure 17 shows the light source and collimating system for the laboratory Scatometer. An aperture for controlling beam diameter is included in the collimating lens mount. The beam splitter is a 6 cm (2.5 in.) square cover glass. The beam monitor detector is positioned to monitor only that portion of the beam passing through the aerosol chamber. The light source is a 100-watt zirconium arc device (manufactured by George W. Gates and Co., Franklin, New York). The spacing of the lenses and other optical elements is adjusted to provide maximum beam power for a given pin hole and beam diameter size. A 100-watt source was required in order to produce sufficient beam power. A collimation angle of 0.16 degrees was obtained.

Recommendations for Optical Design Improvement

Two improvements are recommended in the current design.

1. The collimating and focusing lenses should be free from imperfections that cause background scattering. A decrease in background scattering will allow increased accuracy in scattering measurements.

2. Single element lens should be used. Background scattering is proportional to the number of surfaces. Achromatic lens are not necessary as the device operates well with monocromatic light. Inexpensive spherical lens appear suitable.

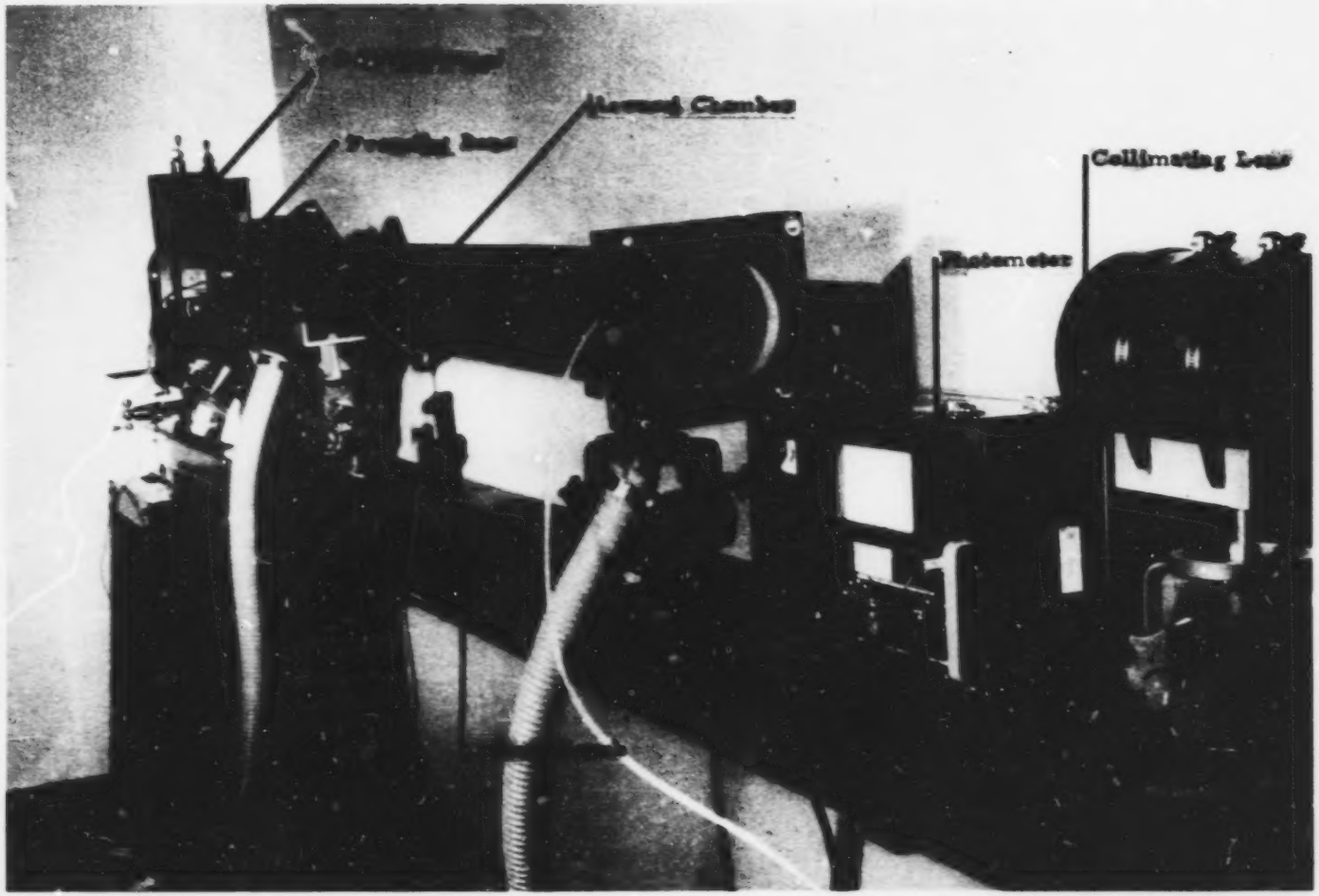

Figure 15. Scatometer and aerosol test chamber

Preceding page blank

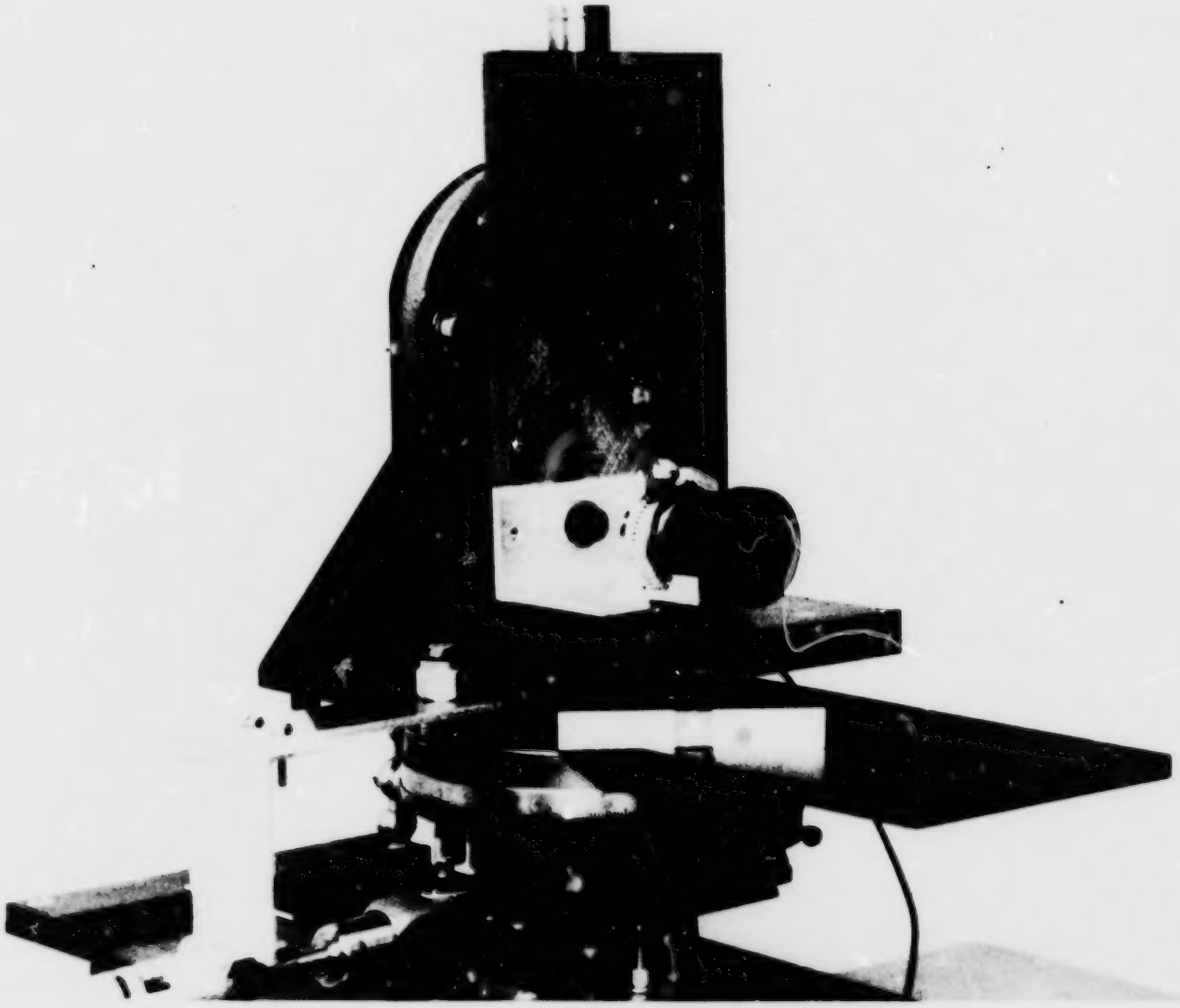

76-340

Figure 16. Detector and crossfeed mounting

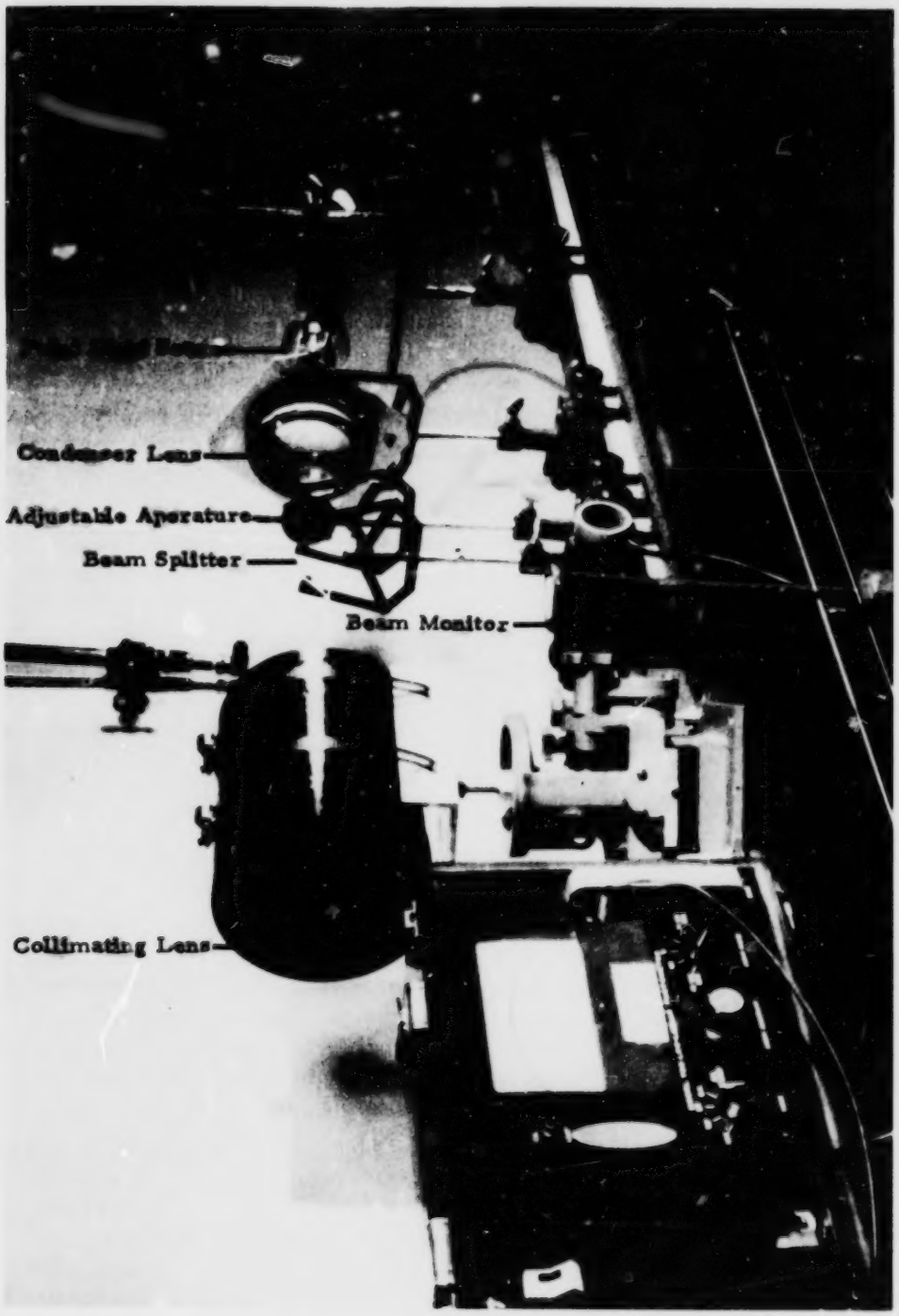

75-563

Figure 17. Scatometer light source

Preceding page blank

SCATOMETER EXPERIMENTS

Two sets of scattering experiments were conducted. The experiments in Set 2 were repeats of Set 1 and generated data on the repeatability of the measurements. Set 1 results were studied and improvements made in experimental technique. Set 2 results are more accurate.

Characteristics of the aerosols tested are indicated in Table 4. The desired opacity and the method for size distribution determination are also given. Tabulation of experimental conditions and results are provided in Appendix A.

Experimental Data Normalization

In order to simplify comparisons of Scatometer results, all measurements are normalized. The normalization corrects for intensity drift of the light source and changes in aerosol concentration. Rate measurements were also made of sedimentation in the test chamber and deposition on the windows. The maximum change in window transmittance caused by deposition was 3/4 percent. Beam intensity changes were typically less than 2 percent and aerosol concentration changed less than 10 percent over the 2 to 4 hour test period. A change in beam intensity is particularly critical because with a transmittance of 90 percent, a 2 percent change becomes a 20 percent error in opacity. The methods for normalizing the data are given in Appendix B.

Experiments, Set 1

The aerosols used in the first set of Scatometer experiments are described in Table 4. During these initial experiments, methods for producing and measuring aerosols were developed. Results from the first set of experiments indicated that the Scatometer technique performed as expected and that the various mass, size distribution, and light scattering data were reasonable and consistent. The direct aerosol size distribution measurements were checked by comparison of the measured opacity to that calculated from the known refractive index, the observed size distribution, and aerosol mass concentration.

Results also indicated that additional size distribution and aerosol concentration measurements would be valuable. Aerosol samples for microscope or SEM examination were not taken on every test. When they were taken, they were often taken only at the aerosol chamber inlet. The size determinations for the 0.5 μm 22 percent opacity, and 2 μm 7 percent opacity PSL aerosols were inferred from opacity and the Set II tests with the same particle size. The size distribution for 3 μm ammonium fluorescein aerosol was based only on the SEM measurements.

TABLE 4

SIZE DISTRIBUTIONS TO SHOW SCATOMETER FEASIBILITY

Aerosol Particle Diameter	Opacity (1.8 m path)	Type of Distribution	Method Of Determining Size Distribution
0.5 μm	22%	PSL, polydisperse	Scanning electron microscope
0.5 μm	14%	PSL, polydisperse	Scanning electron microscope
2.0 μm	14%	PVL, monodisperse	Optical microscope
2.0 μm	7%	PVL, monodisperse	Optical microscope
6.0 μm	5%	PSL, monodisperse	Optical microscope
~3.0 μm	10-25%	Ammonium fluorescein, polydisperse	Impactor
~1.0 μm	11-25%	Ammonium fluorescein, polydisperse	Impactor

PSL = Polystyrene latex

PVL = Polyvinyltoluene latex

Filter mass data were limited for the 2 μm ammonium fluorescein mass only 1 sample was collected. The 1 μm ammonium fluorescein mass determination was poor because of large measurement errors. The 5.7 μm aerosol suffered from agglomeration and about 50 percent settle-out in the aerosol chamber. In perspective, the additional errors of 10 to 20 percent introduced by these problems were not serious.

Experiments, Set 2

The second set of Scatometer evaluation experiments repeated the Set 1 tests for the purpose of estimating reproducibility and improving aerosol measurement techniques. The major improvement was the increased precision and number of data points obtained. The following additions were made to the experiments: (1) the test plan was modified to provide duplicate measurements (2) more attention was given to producing monodisperse aerosols (3) more complete size distribution measurements were made, and (4) aerosol particle structure was examined using a scanning electron microscope (SEM). Selected Set 1 aerosol samples were also examined with the SEM.

The Set 2 results again confirmed the theoretical calculations. The agreement between the first and second set of experiments was good and indicated overall consistency of the experimental work.

EXPERIMENTAL RESULTS

Tables 5 and 6 contain summaries of the experimental results in numerical form. These tables present mass concentration determined by the Scatometer algorithm versus forward scattering angle and aerosol parameters including composition, opacity, size distribution, true mass concentration, and Scatometer to true mass ratio. Note that all values have been corrected to a constant aerosol density and source brightness for easier comparison. An error estimate associated with each measurement is listed below or next to each entry. The opacity and mass values are averages of two to four measurements; the error has been estimated as the unbiased standard deviation of the individual measurements divided by the square root of the number of measurements, N_m, so that

$$\text{error in percent} = \frac{100\sqrt{\frac{\Sigma(X_i - \bar{X})}{N_m - 1}}}{\sqrt{N_m}\,\bar{X}}$$

X_i = the i^{th} value

$\bar{X}$ = average of measurements

Table 5. SCATOMETER EXPERIMENTAL RESULTS, SET 1

TEST NO.	NOMINAL PARTICLE DIAMETER (μm)	SIZE DISTRIBUTION		PARTICLE COMPOSITION	MEASURED OPACITY (1-T)	AEROSOL MASS INDICATED BY SCATOMETER (mg/m^3)					AEROSOL MASS COLLECTED ON FILTER (mg/m^3)	EXPERIMENTAL RESPONSE OF SCATOMETER/ TRUE MASS* @ 3/4°
		d_g (μm)	σ_g			1/2°	3/4°	1°	2°	3°		
1-1	0.5	1. (30)	2 (15)	PSL	0.125 (<0.5)	28 (<0.5)	28 (<0.5)	26 (4)	26 (3)	25 (15)	11 (2)	2.4
1-2	0.5	1.3 (30)	2 (25)	PSL	0.24 (6)	72 (19)	--	69 (5)	65 (<0.5)	65 (2)	21 (1)	3.4[c]
1-3	2.0	2.[b] (10)		PVL	0.07 (9)	27 (24)	30 (6)	29 (2)	27 (1)	25 (7)	28 a	1.08
1-4	2.0	1.8[b] (20)		PVL	0.13 (6)	49 (2)	47 (7)	47 (7)	43 (2)	35 (1)	47 (1)	1.00
1-5	5.7	1.2[b]		PSL	0.13 (5)	139 (4)	--	119 (3)	71 (15)	46 (1)	142[d] (2) 77[e] (4) 123[f]	1.12[c]
1-6	1	1. (30)	4 (25)	Am. Fl.	0.23 (0.5)	68 (1)	--	65 (2)	57 (<0.5)	54 (2)	42 (12)	1.85[c]
1-7	3	3. (25)	3.5 (14)	Am. Fl.	0.13 (<0.5)	49 (6)	49 (1)	50 (2)	46 (1)	42 (5)	42 (7)	1.16

* True mass as determined by filter sampling.
( ) Number in parentheses is estimated error range in %.
a) Only one mass sample available
b) Ratio of singlet mass to mass in multiplets
c) @ 1/2°
d) Scattering chamber inlet
e) Scattering chamber outlet
f) Best estimate
g) 1.8 meter path

Table 6. SCATOMETER EXPERIMENTAL RESULTS, SET 2

TEST NUMBER	NOMINAL PARTICLE DIAMETER	SIZE DISTRIBUTION		PARTICLE COMPOSITION	MEASURED OPACITY (1-T)	AEROSOL MASS INDICATED BY SCATOMETER (mg/m^3)					AEROSOL MASS COLLECTED ON FILTER (mg/m^3)	EXPERIMENTAL RESPONSE OF SCATOMETER/TRUE MASS* @3/4°
		d_g	σ_g			1/2°	3/4°	1°	2°	3°		
2-1	0.5	0.75 (13)	2 (20)	PSL	0.14 (<1)	25 (15)	29 (1)	28 (6)	27 (1)	28 (1)	14 (1)	2.06
2-2	0.5	0.74 (11)	1.7 (18)	PSL	0.20 (<1)	49 (1)	44 (1)	44 (1)	44 (3)	43 (6)	20 (2)	2.18
2-3	2.0	1.4[a] (11)		PVL	0.083 (9)	41 (5)	40 (3)	39 (<1/2)	36 (4)	33 (1)	32 (5)	1.25
2-4	2.0	1.1[a] (14)		PVL	0.13 (2)	68 (1)	67 (<1/2)	67 (5)	62 (<1/2)	57 (<1/2)	58 (1)	1.15
2-5	5.7	4.0[ab] (10) 5.6[ac] (8)		PSL	0.081 (2)	93 (3)	93 (1)	90 (1)	72 (<1)	51 (1)	101[b] 76[c] 88[d]	1.07
2-6	0.6	0.57	2 (10)	Am. Fl.	0.14 (5)	32 (3)	29 (<1/2)	27 (4)	26 (4)	27 (8)	13 (6)	2.29
2-7	3	2.8 (14)	3.9 (8)	Am. Fl.	0.23 (<1/2)	129 (2)	129 (1)	128 (1)	117 (<1/2)	106 (1)	91 (5)	1.42

a) Ratio of singlet mass to multiplet mass
b) Chamber inlet
c) Scattering chamber outlet
d) Best estimate
* True mass as determined by filter sampling
( ) Number in parentheses is estimated error range in %

This error reflects random variations and does not include systematic effects. Note that the error at 1/2° for small aerosols often differs markedly from the error at 3/4°. This effect is probably due to the high background scattering associated with poor quality lenses. The errors associated with the size distribution parameters are estimates based on counting statistics in the cases where particles were counted optically, on statistics calculated from impactor measurements, and on agreement between measured opacity and that calculated from impactor measurements, and on agreement between measured opacity and that calculated from the size distribution. The errors below the Scatometer mass entries are the scattered light intensity errors at the corresponding angle. The errors in the Scatometer mass value, which are not shown, are equal to the root mean square of the opacity and intensity errors. The large ammonium fluorescein aerosol particles have an uncertainty in specific gravity that is not included in these errors.

The Scatometer-to-filter mass ratio indicates the overall accuracy of the Scatometer technique. The scattering at 3/4° was used in computing this ratio when available (some 1/2° values were used) because high background appeared to lower the reliability of the 1/2° measurements, particularly for small aerosols for which forward scattering is weak.

The Scatometer-to-true mass concentration ratios are shown graphically in Figure 18. The solid curve indicates response for a monodisperse polystyrene aerosol for rough comparison. Note that many of the aerosols are polydisperse. Scatometer response follows the theoretical predictions well except at the 1.3 μm point. In spite of the size distribution uncertainty (see Table 4), an experimental error appears likely. Large particle response is the most accurate.

Figure 19 illustrates the experimental transmissometer response to the opacity of the aerosols tested. The transmissometer response has been assumed to be directly proportional to the optical depth and the constant of proportionality selected such that the transmissometer measurements in the 0.7 to 1 μm range are the same height as the Scatometer response. This normalization allows easy comparison of the flatness of the two responses. Only relative curvatures are important because constant biases can be calibrated out in the field. The typical response fall off is evident for larger particles.

Figure 20 presents the ratio of experimental Scatometer response to predicted theoretical response and indicates the accuracy with which the experimental data agree with theoretical calculations. Points on the $y = 1.0$ line indicate exact agreement. The error bars indicate approximately the 95 percent confidence limits. These limits are based on the uncertainities in light scattering data, the filter aerosol concentration

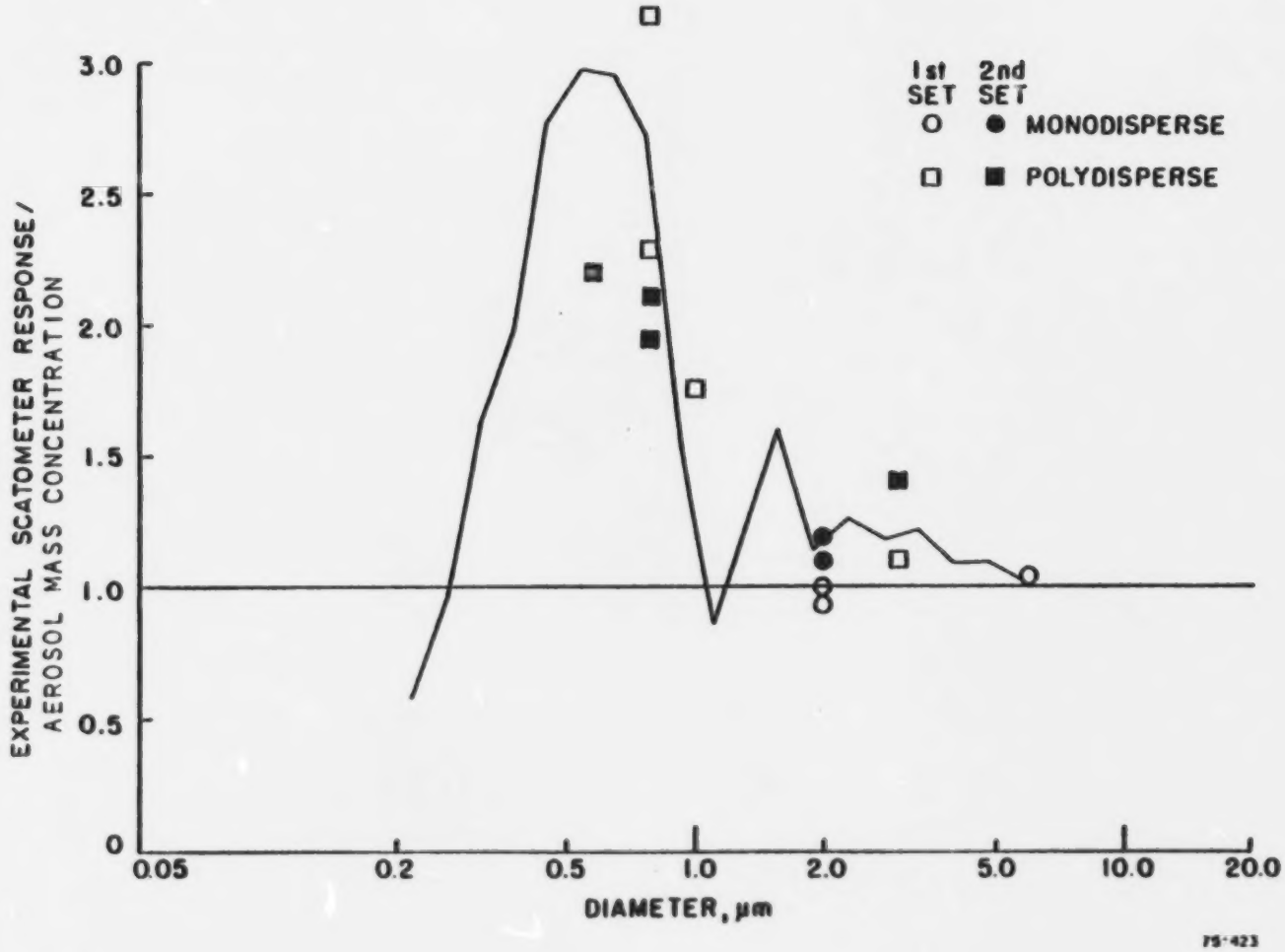

Figure 18. Experimental Scatometer response per unit mass concentration of aerosol as a function of particle size

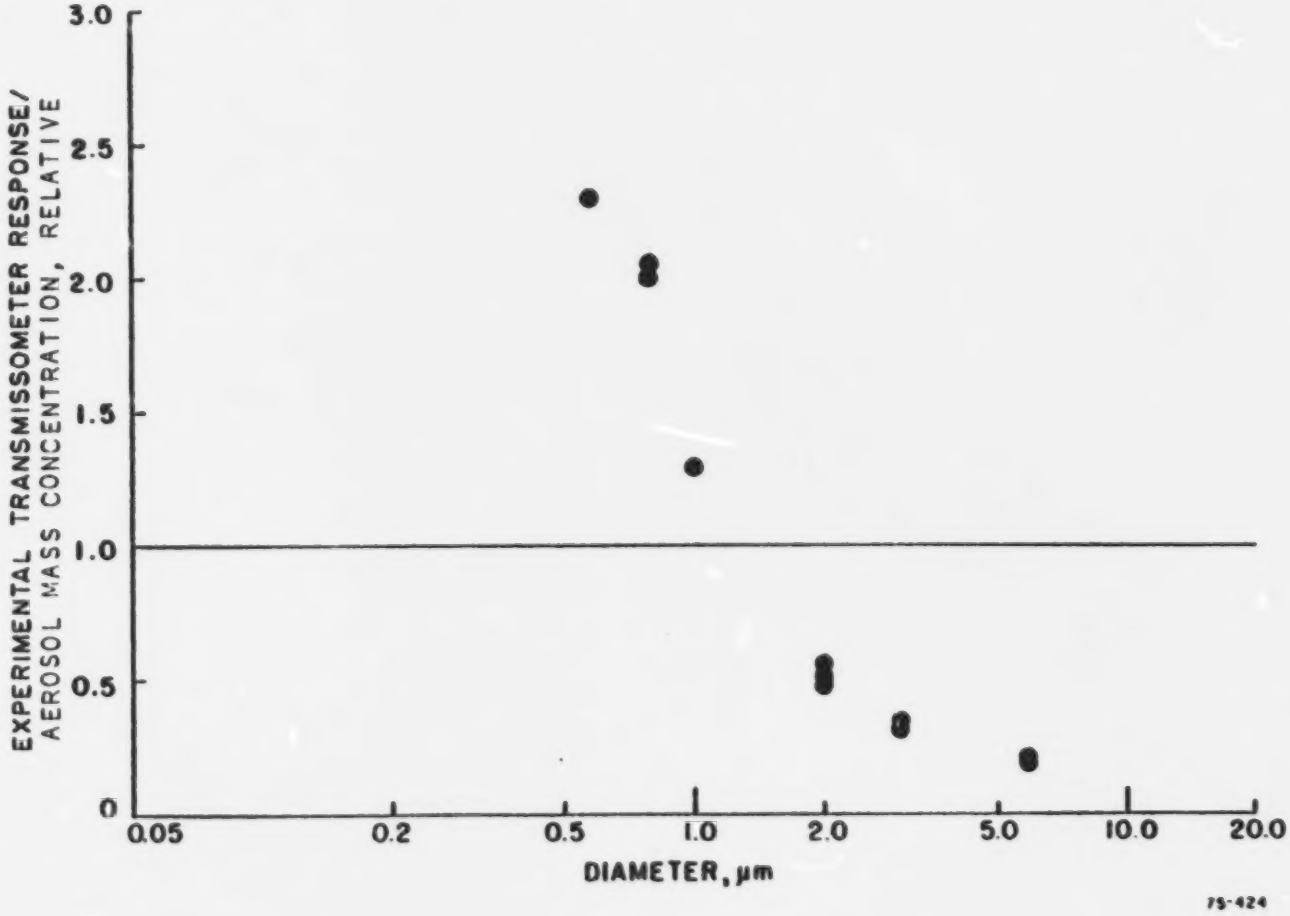

Figure 19. Relative experimental transmissometer response (optical depth per unit mass concentration of aerosol) as a function of particle size

data, and the size distribution data. In some cases, particularly where no direct measurement was made of size distribution, uncertainties were estimated from procedures involved and not simply calculated explicitly from measured points. The limits basically reflect expected random errors. Theoretical-to-experimental response ratios that are close to 1 indicate good agreement of experimental results with theory.

No attempt was made to model theoretically the effect of doublets and larger multiplets for the 2 and 5.7 μm aerosols. Calculation of these effects are beyond the scope of the present contract. The high percentage of multiplets may contribute to some of the low results.

Generation of consistent ammonium fluorescein aerosols at 2.8 and 3.0 μm was difficult and the errors may be greater than those shown by the error limits. The point at 1.3 μm (Figure 20) is doubtful and, therefore, shown dashed.

The points near 0.75 and 6 μm have small errors and show excellent correlation with theory. The small error limits indicate that data obtained, particularly measured opacity and size distribution data, are consistent. The larger limits on the 6 micron points reflect primarily the uncertainty in aerosol concentration caused by particle fallout within the scattering chamber.

A number of points have asymetrical error limits. This result is primarily due to the variation in calculated Scatometer response with particle size and polydispersity. For example, response may change more rapidly with decreasing particle size than with increasing size. The wide error bands for the 4 points at 2 μm are also due to response variation. At 2 μm a small uncertainty in size results in a large uncertainty in the predicted response because the theoretical response changes very rapidly with diameter (see Figure 18). It is likely that the low response is partly an artifact of the theoretical calculations.

The theoretical calculations used in these data were made for monochromatic light at 0.56 μm, the center of the photopic curve, while the experiments were made using a detector with a photopic response. The error introduced by the band width is negligible except for the 2 μm aerosols where it may be as large at 4 percent. This error has been included in the results of Figure 20.

Figures 21 through 25 show photomicrographs that are typical of the aerosols generated in this study.

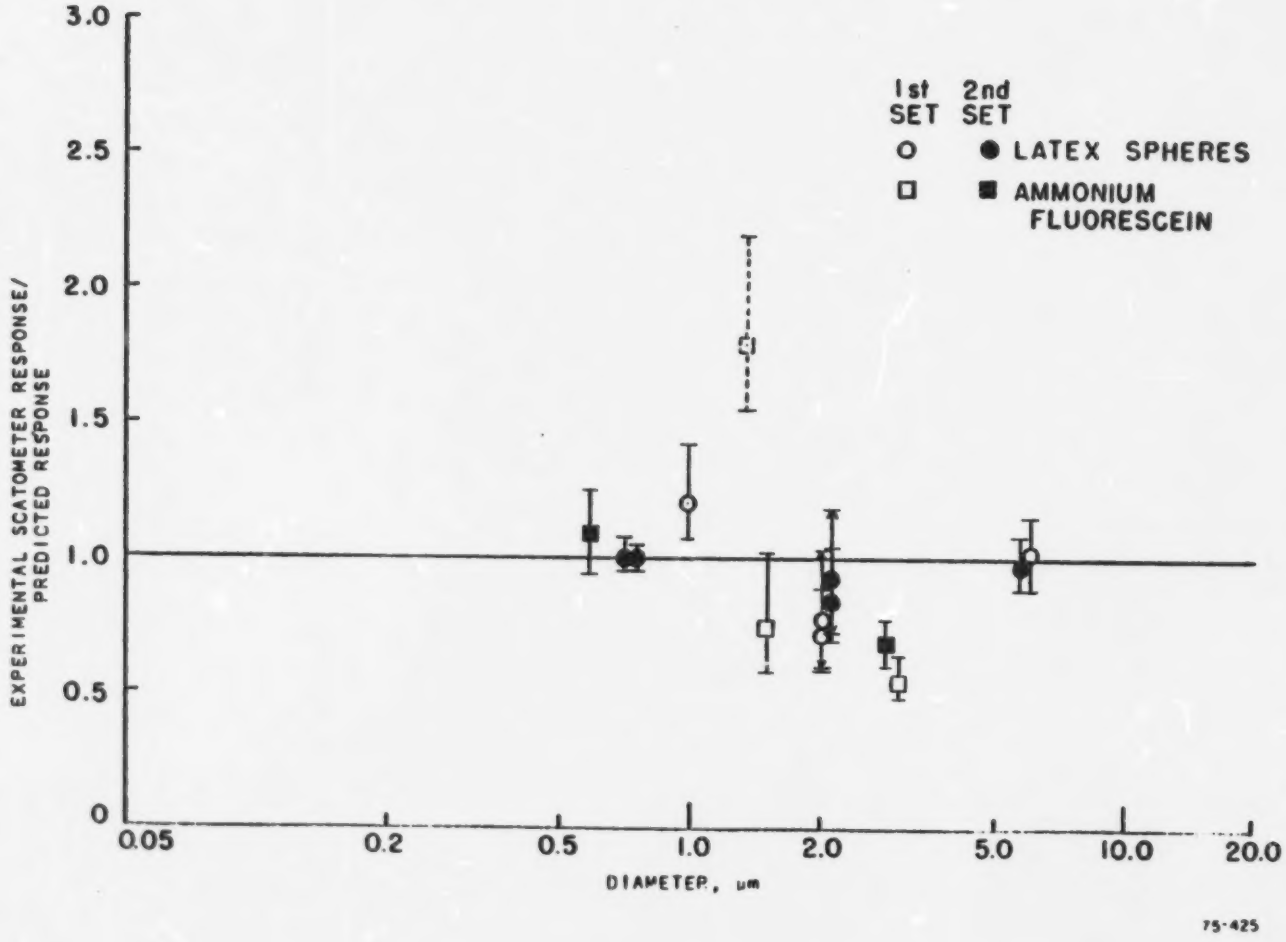

Figure 20. Experimental Scatometer response per predicted response as a function of particle size

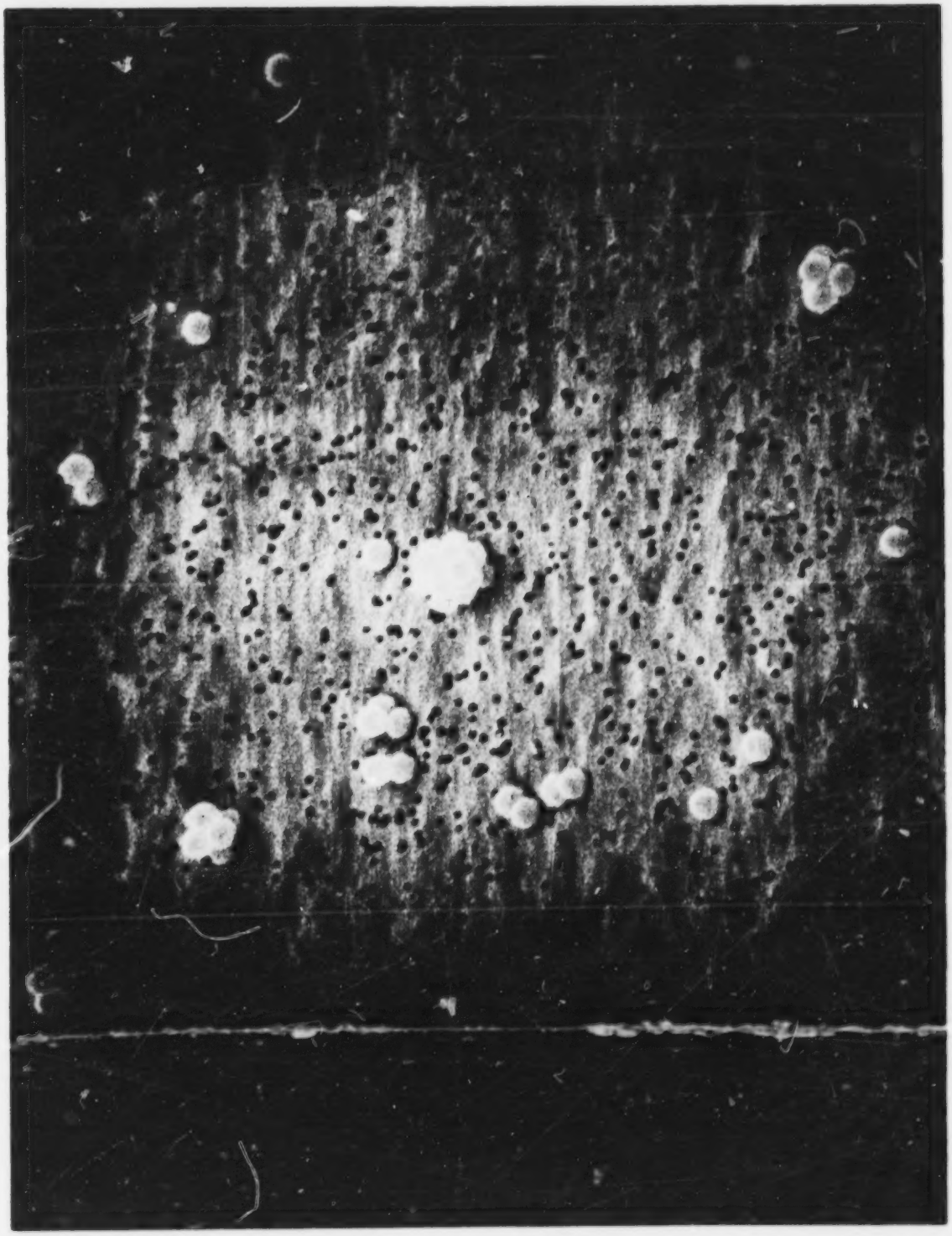

76-341

Figure 21. Polystyrene latex aerosol particles, 1/2 μm diameter

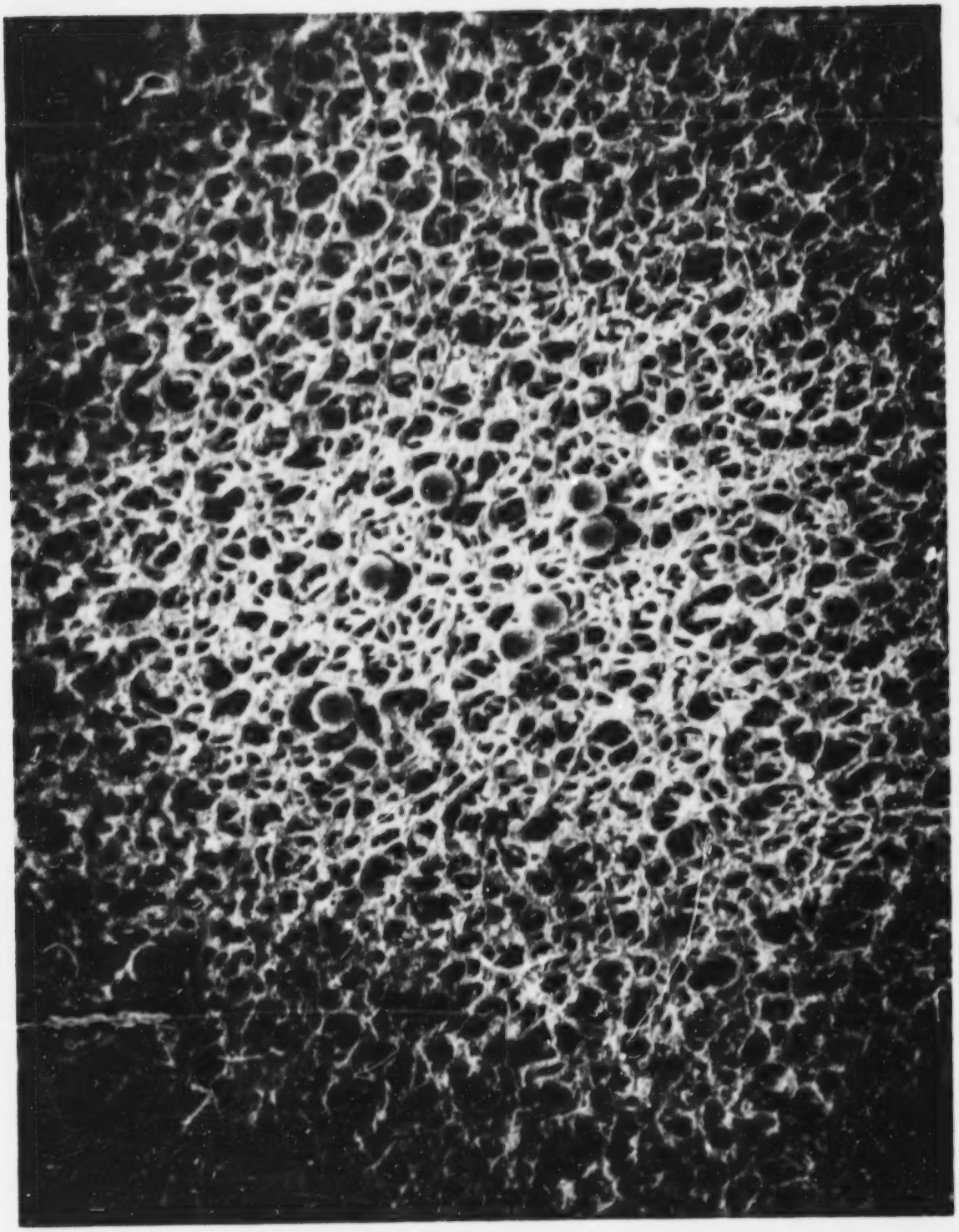

76-342

Figure 22. Polyvinyltoluene latex aerosol particles 2 μm diameter

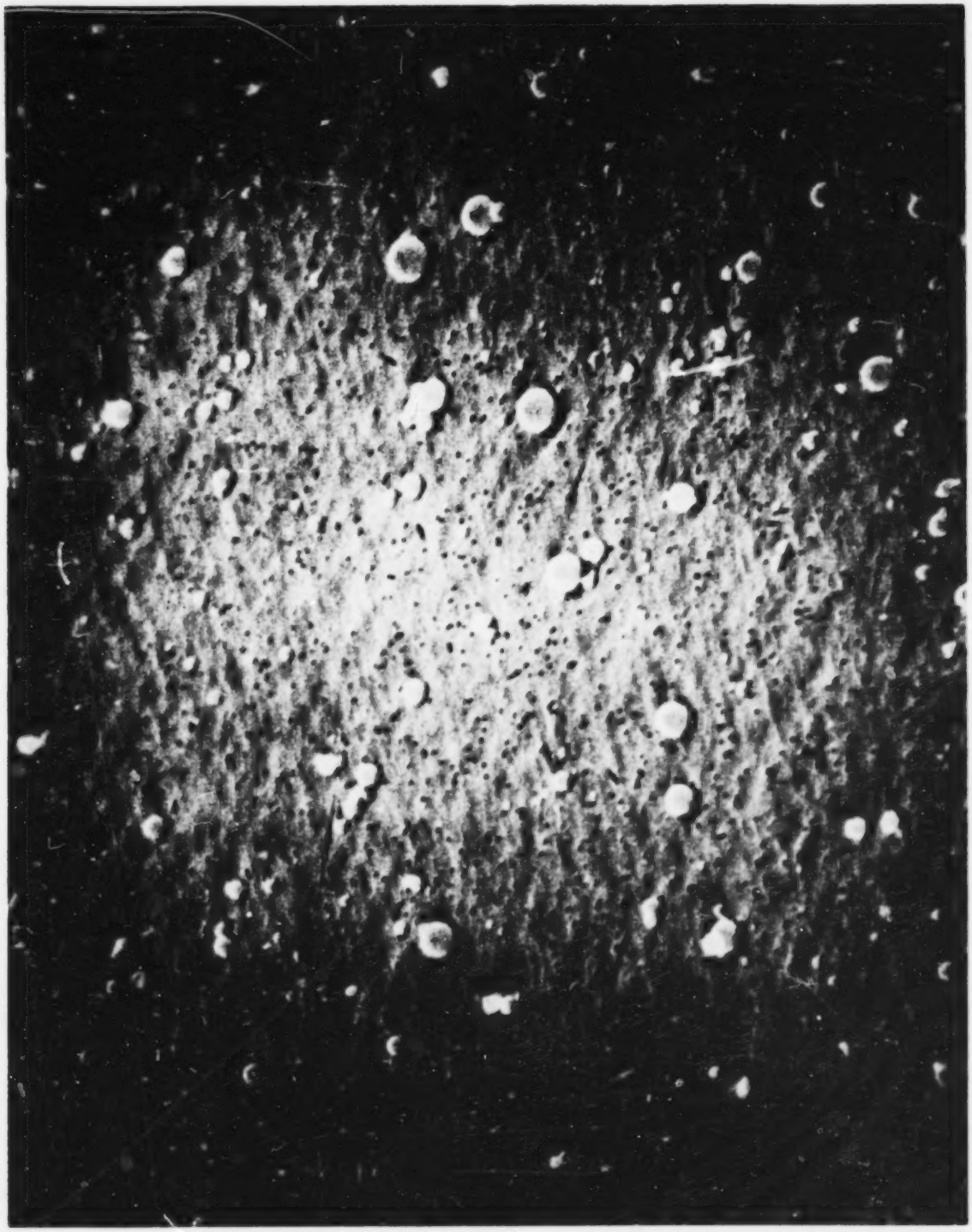

76-343

Figure 23. Ammonium fluorescein aerosol particles, 0.57 μm volume median diameter

Preceding page blank

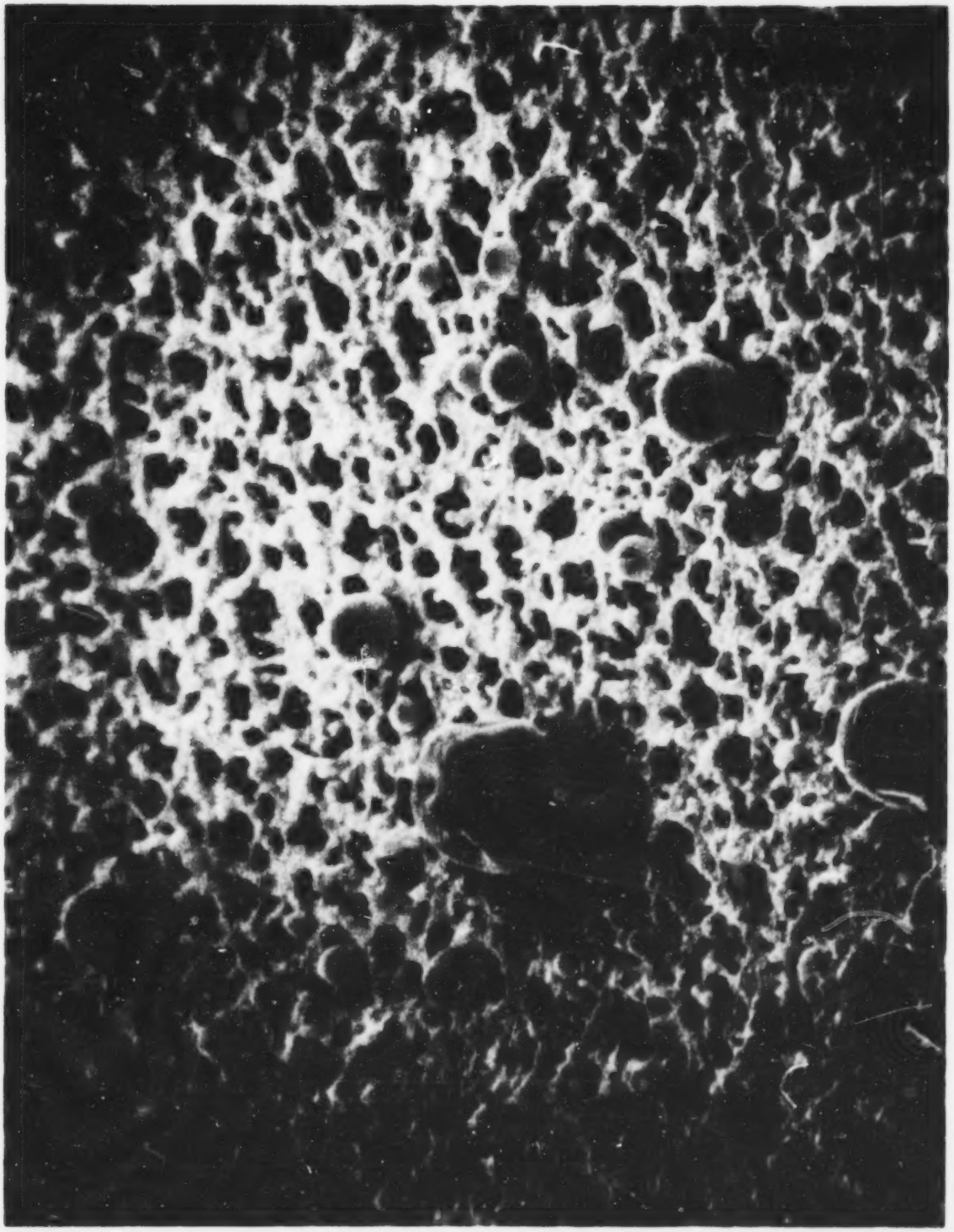

76-344

Figure 24. Ammonium fluorescein aerosol particles, 3 μm volume median diameter, Experimental Set 1

Preceding page blank

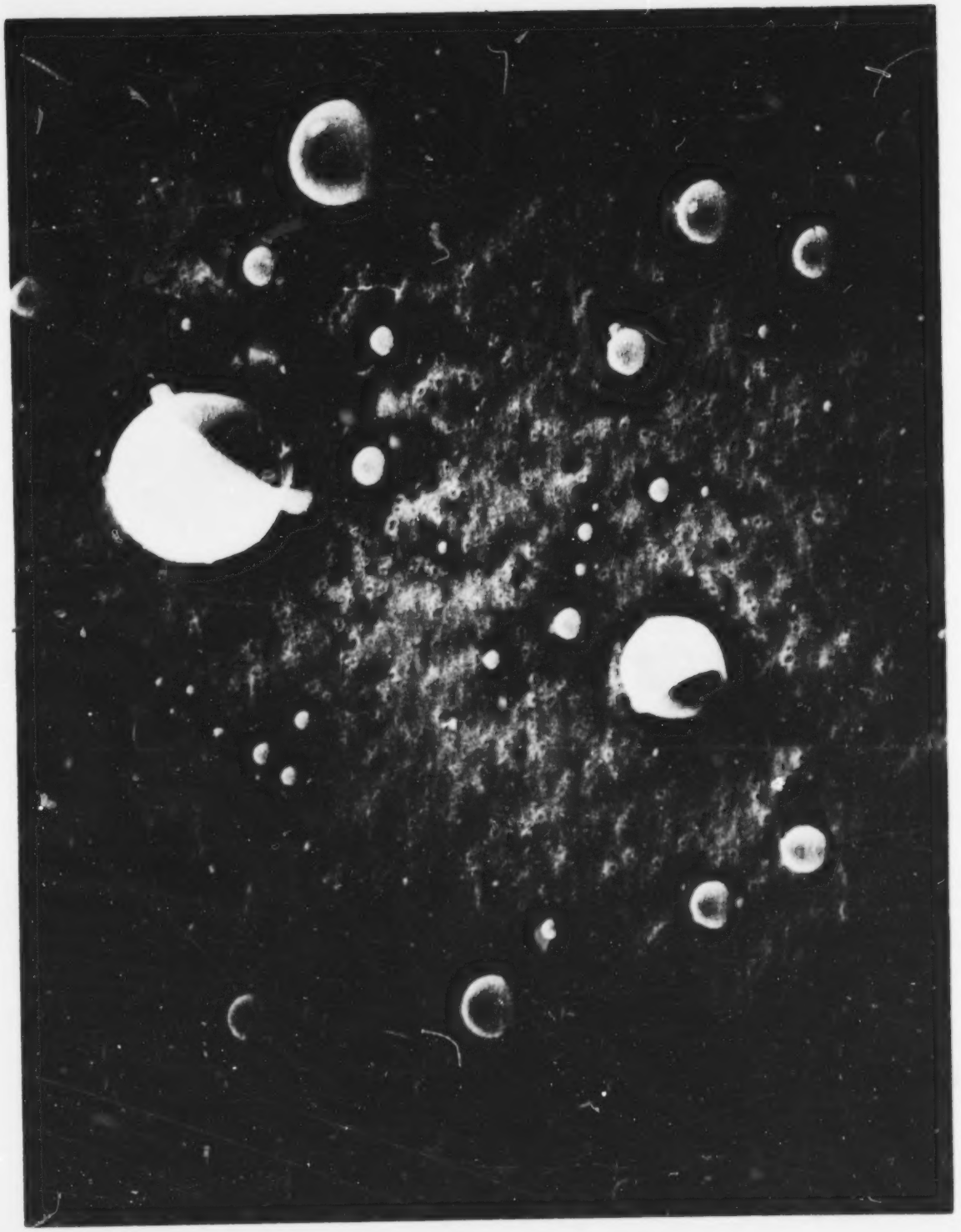

76-345

Figure 25. Ammonium fluorescein aerosol particles, 2.8 μm volume median diameter, Experimental Set 2

Figure 21 shows 0.5 μm diameter spheres from Set 2 experiments at an aerosol concentration of 20 mg/m^3. Some agglomeration is evident. The median volume diameter measured from SEM photographs is 0.74 μm.

Figure 22 shows 2 μm diameter PVL spheres from the lower opacity experiment, Set 2. Again some doublets are apparent. Figure 23 shows Set 2 small ammonium fluorescein aerosol. The particles are spherical.

Figures 24 and 25 show Set 1 and 2 large ammonium fluorescein aerosol particles respectively. Both aerosols were generated under similar conditions except for initial concentration of the ammonium fluorescein solution, which was 3 and 9 percent respectively. The large particles of both aerosols are nonspherical and appear to have formed a crust while drying. The Set 2 particles appear to have formed a thin shell which often cracked after collection on the filter. It appears likely that the low response indicated in Figure 20 is associated with the odd structure of these aerosols.

The nearness of most points to a theoretical-to-experimental ratio of 1 in Figure 20 indicates good agreement between theoretical prediction and experimental results. The inclusion of one within most error limits strongly supports the hypothesis that the theoretical calculations accurately predict Scatometer response and that the differences are the result of random experimental variations. Particularly convincing are those points near 0.7 and 6 μm diameter with very small error limits. The experiments also indicate that the Scatometer technique is insensitive to particle shape. Many aerosols tested, particularly the 0.5 and 2 μm diameter aerosols (see Figure 21, and 22) contained a large fraction of their mass in nonspherical particles, i.e., doublets, triplets, and multiplets; yet the experimental response correlates well with the theoretical calculations for spherical particles. Some shape dependence appears indicated by the low response for the large ammonium fluorescein aerosols. Unfortunately, other irregularities were also present in these experiments, and a firm conclusion cannot be made.

SECTION 6

REFERENCES

1. Shifrin, K. S. and A. Y. Perelman. Tellus 18. pp. 566-572. 1966.

2. Gunther, R. Staub in English 33. pp. 345-352. 1973.

3. Livesey, P. J. and F. W. Billmeyer, Jr. J. Colloid Interface Sci., 30, pp. 447-472. 1969.

4. Meehan, E. J. and A. E. Gyberg. Appl. Opt., 12. pp. 551-554. 1973.

5. Dave, J. V. Subroutines for Computing the Parameters of the Electromagnetic Radiation Scattered by a Sphere. Rep. No. 320-3237, IBM Scientific Center, Palo Alto, California. 1968.

6. Davis, P. J. and P. Rabinowitz. Numerical Integration. Blaisdell Publishing, Waltham, Massachusetts. pp. 166-170. 1967.

7. Ralston, A. and H. S. Wiff. Numerical Methods for Computers, Wiley, New York. pp. 133-144. 1967.

8. Raabe, Otto G. J. Amer. Ind. Hyg., 29. pp. 439-443. 1968.

9. BGI, Inc., Waltham, Mass.

10. Retec Development Laboratory, Portland, Oregon.

APPENDIX A

EXPERIMENTAL DATA LOGS

This appendix discusses the 14 individual scattering experiments. The heading "Size Distribution Versus Opacity" refers to calculation of the opacity from the measured size distribution and aerosol concentration or vice versa. The agreement between an inferred size distribution and measured parameters is a good check on the accuracy of the mass and size distribution measurements, particularly since the opacity measurement is reliable. The size distribution errors given are 95 percent confidence limits. The 0.5 μm PSL and ammonium fluorescein aerosol size distributions were fit to a lognormal volume distribution. Since the distributions may differ from an exact lognormal distribution, some error may occur in calculating theoretical response. This error is not likely to exceed 10 percent and is probably less than 5 percent.

Preceding page blank

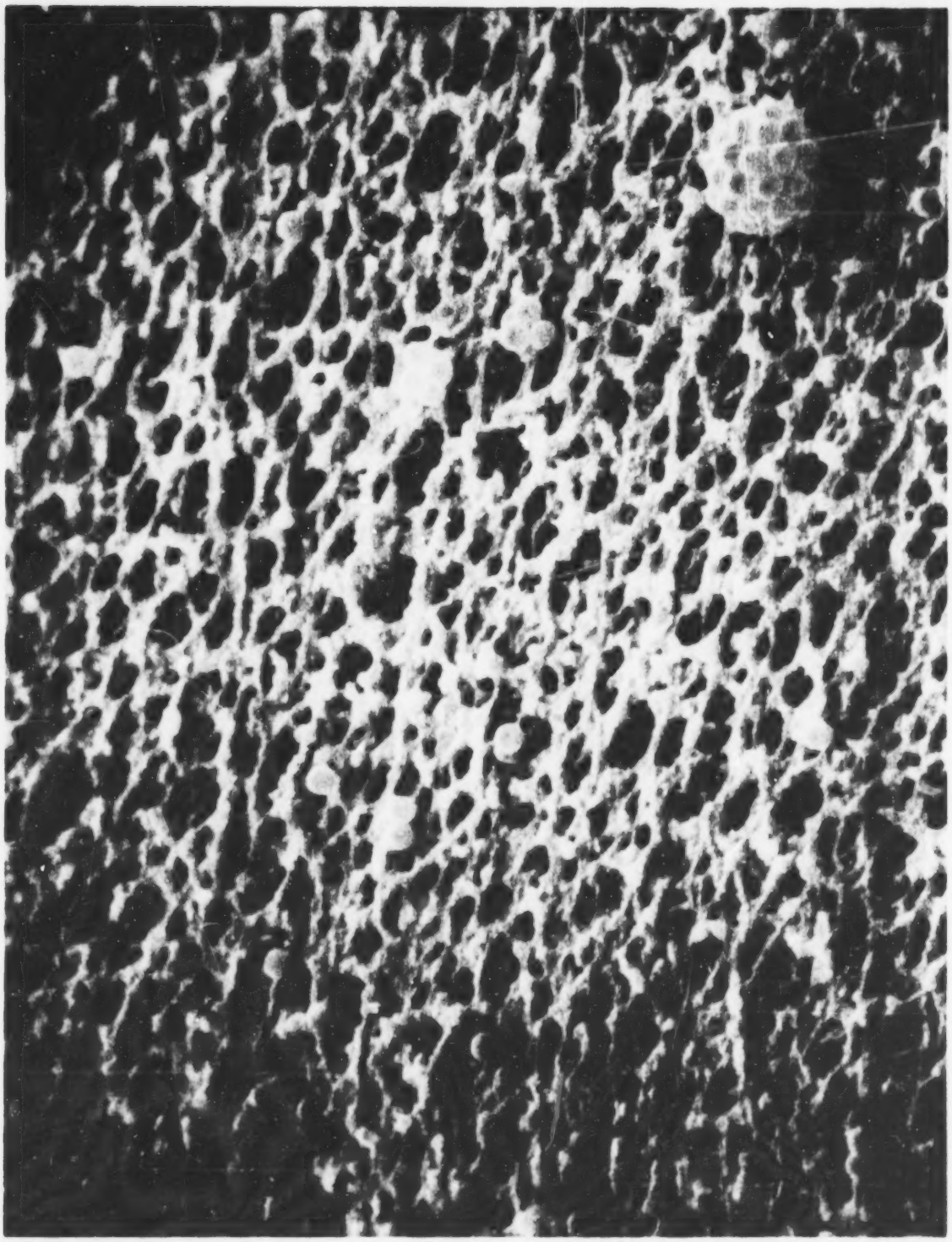

76-346

Figure A-1. Set 1, test 1 aerosol SEM photomicrograph

EXPERIMENTAL DATA LOG

SET: 1 **TEST:** 1 **DATE:** 6/27/75

AEROSOL MATERIAL: 0.5 μm PSL

MEASURED OPACITY: 12.5 %

SIZE DISTRIBUTION: Determined by counting and opacity measurements.

VOLUME MEDIAN DIA.: $1\ \mu m\ ^{+0.6}_{-0.4}$

GEOMETRIC STD. DEV.: $1.75\ ^{+0.6}_{-0.3}$

MEASURED MASS CONCENTRATION (by filter) (mg/m^3):

INLET: 11.6 ±3%

OUTLET: 12.0 ±1.5%

NEBULIZER AND PRESSURE: Collison @ 19 psi

NEBULIZER FLUID CONCENTRATION: 1%

SIZE CALCULATED FROM OPACITY AND MASS MEASUREMENTS: Median diameter between 0.64 and 0.8 μm

PHOTOMICROGRAPH MEASUREMENTS: Counting statistics appear below.

Diameter (μm)	Cumulative Mass (%)	No. of Particles or Agglomerates
0.5 (Singlets)	10	21
0.63 (Doublets)	14	4
0.72 (Triplets)	22	6
0.7-1	49	8
1-1.3	49	0
1.3-1.8	56	1
1.8-2.3	100	2
Total		42

This size distribution fits a lognormal distribution with d_g = 1.15μm and σ_g = 1.75.

SET 1, TEST 1 (CONT.)

COMMENTS: Size distribution was determined from SCM photomicrographs and comparison of measured and calculated opacity. Photomicrographs were taken of four filter areas, one of which was shown in Figure A-1. Note the large agglomerates. The counting statistics from the four photomicrographs are above.

The counting and opacity size distribution show a significant difference. This may be due to counting statistics, agglomeration of particles on the filter, or both, and did not occur in the Set 2 experiments. The filter hypothesis is supported by the fact that a radioactive ionizer was installed for the Set 2 experiments. The Aerosol Generator parameters were not significantly different between Set 1 and 2. This again supports the agglomeration hypothesis. The experimental-to-theoretical response ratio is too high (see Figure 20) and probably reflects an experimental error as the Set 2 runs exhibit excellent agreement with similar aerosol.

EXPERIMENTAL DATA LOG

SET: 1 **TEST:** 2 **DATE:** 5/29/75

AEROSOL MATERIAL: 0.5 μm PSL

MEASURED OPACITY: 24.6%

SIZE DISTRIBUTION: Determined by extrapolation and opacity.

VOLUME MEDIAN DIA.: No optical sample taken.

GEOMETRIC STD. DEV.:

MEASURED MASS CONCENTRATION (by filter) (mg/m^3):

INLET: 21.5 (1 sample)

OUTLET: 21.3 (1 sample)

NEBULIZER AND PRESSURE: Collison @ 5 psi

NEBULIZER FLUID CONCENTRATION: 4%

SIZE CALCULATED FROM OPACITY AND MASS MEASUREMENTS: Corresponds to MMD between 0.64 μm and 0.8 μm.

PHOTOMICROGRAPH MEASUREMENTS: No sample taken.

COMMENTS:

1. Size distribution is quite uncertain. A larger size distribution than Test 1-1 is expected since a 4 percent suspension of latex spheres and lower pressure were used in the nebulizer.

2. An experimental-to-theoretical response ratio compared with the other 0.5 μm diameter aerosols, both Set 1 and 2, is far too high.

3. The above points cast extreme suspicion on the results.

EXPERIMENTAL DATA LOG

SET: 1 **TEST:** 3 **DATE:** 5/19/75

AEROSOL MATERIAL: 2.02 μm PVL

MEASURED OPACITY: 7%

SIZE DISTRIBUTION: Extrapolated from other tests and opacity.

VOLUME MEDIAN DIA.: Filter sample too densely packed for measurement.

GEOMETRIC STD. DEV.:

MEASURED MASS CONCENTRATION (by filter) (mg/m^3):

INLET: 27.9 (1 sample)

OUTLET: same (see Comments)

NEBULIZER AND PRESSURE: Spraying systems 1/4 J1A set up with baffles.

NEBULIZER FLUID CONCENTRATION:

SIZE CALCULATED FROM OPACITY AND MASS MEASUREMENTS: Opacity corresponded closely to a monodisperse aerosol.

PHOTOMICROGRAPH MEASUREMENTS: None.

COMMENTS: Measurements appeared self-consistent. The response appeared to be abnormally low which did not occur in Set 2.

Sedimentation in aerosol chamber was checked by switching the nephelometer from outlet to inlet; none was apparent.

EXPERIMENTAL DATA LOG

SET: 1 TEST: 4 DATE: 6/3/75

AEROSOL MATERIAL: 2.02 μm PVL

MEASURED OPACITY: 12.6%

SIZE DISTRIBUTION: Determined by counting.

VOLUME MEDIAN DIA.: 2 μ

GEOMETRIC STD. DEV.:

MEASURED MASS CONCENTRATION (by filter) (mg/m^3):

INLET: 38.5 and 47.0

OUTLET: 47.0 and 47.3

NEBULIZER AND PRESSURE: Collison @ 25 psi

NEBULIZER FLUID CONCENTRATION: 2%

SIZE CALCULATED FROM OPACITY AND MASS MEASUREMENTS: Consistent with a monodisperse aerosol.

PHOTOMICROGRAPH MEASUREMENTS:

Aerosol Mass Distribution

67% Singlets

23% Doublets

5% Triplets

3% Quads or quints

370 Singlets counted

No significant difference between inlet and outlet.

COMMENTS: Measurements appear self-consistent.

EXPERIMENTAL DATA LOG

SET: 1 **TEST:** 5 **DATE:** 6/13/75

AEROSOL MATERIAL: 5.7 μm PSL

MEASURED OPACITY: 13%

SIZE DISTRIBUTION: Determined by counting.

VOLUME MEDIAN DIA.: 5.7 μm

GEOMETRIC STD. DEV.: See Photomicrograph Measurements

MEASURED MASS CONCENTRATION (by filter) (mg/m^3):

INLET: 142 $\pm$2% AVERAGE: 109

OUTLET: 77 $\pm$4%

NEBULIZER AND PRESSURE: Retec X-70/N @ 15 psi

NEBULIZER FLUID CONCENTRATION: 7%

SIZE CALCULATED FROM OPACITY AND MASS MEASUREMENTS: The measured opacity corresponds to a monodisperse distribution @ 126 mg/m^3 conc.

PHOTOMICROGRAPH MEASUREMENTS:

	Inlet		Outlet	
	% by Weight	No. Counted	% by Weight	No. Counted
Singlets	44	45	58	46
Doublets	30	15	27	11
Triplets	6	2	15	4
Quads and Strings	20	5	0	0

COMMENTS: Considerable settle out occured in the aerosol chamber. The concentration in the beam was estimated to be 123 mg/m^3, midway between the inlet and average values. The beam concentration is higher than the average since particles which settle out from the beam tend to be replaced from those settling down from above the beam. The estimated concentration is supported by the opacity measurement. The data appear trustworthy.

EXPERIMENTAL DATA LOG

SET: 1 **TEST:** 6 **DATE:** 6/19/75

AEROSOL MATERIAL: Ammonium fluorescein and uranine.

MEASURED OPACITY: 23%

SIZE DISTRIBUTION: Determined by impactor.

VOLUME MEDIAN DIA.: $1.0\ \mu m\ ^{+0.3}_{-0.2}$

GEOMETRIC STD. DEV.: $3.8\ ^{+0.6}_{-0.5}$

MEASURED MASS CONCENTRATION (by filter) (mg/m^3):

INLET: 37.8 and 36.0

OUTLET: 52.3

NEBULIZER AND PRESSURE: Retec X-70/N @ 25 psi

NEBULIZER FLUID CONCENTRATION: 1.6%

SIZE CALCULATED FROM OPACITY AND MASS MEASUREMENTS: Agrees very well with measured size distribution.

PHOTOMICROGRAPH MEASUREMENTS: None.

COMMENTS: This run was performed unsupervised by a technician. The nebulizer solution was improperly prepared and was a mixture of ammonium fluroescein in solution and acid fluorescein (uranine) in suspension. The aerosol produced was a mixture of these two compounds. Very likely, the large particles were non-spherical; no optical sample was available. The tails of the distribution differed markedly from log normal. The aerosol density is uncertain as the specific gravity of ammonium fluorescein is 1.35 and acid fluorescein between 1.48 and 1.53.* Considering problems encountered, the experiment results appear to agree well with the theoretical prediction.

* Stöber, Werner and Flachsbart, Hermann, Atmos. Envir., 7, pp. 737-748, 1973.

EXPERIMENTAL DATA LOG

SET: 1 **TEST:** 7 **DATE:** 6/27/75

AEROSOL MATERIAL: Ammonium Fluorescein

MEASURED OPACITY: 12.5%

SIZE DISTRIBUTION: Estimated from latter experiments and SEM pictures

VOLUME MEDIAN DIA.: 3 μm $^{+.8}_{-.6}$

GEOMETRIC STD. DEV.: 3.5 $^{+1.4}_{-0.6}$

MEASURED MASS CONCENTRATION (by filter) (mg/m^3):

INLET: $39.5 \pm 3\%$

OUTLET: $45.2 \pm 1\%$

NEBULIZER AND PRESSURE: Retec X-70/N @ 10 psi

NEBULIZER FLUID CONCENTRATION: 3.3%

SIZE CALCULATED FROM OPACITY AND MASS MEASUREMENTS: Consistent with estimated size distribution.

PHOTOMICROGRAPH MEASUREMENTS: See below.

COMMENTS: Size distribution was estimated from SEM photographs and comparison with Set 2 aerosol results. An impactor sample was taken, but the data proved to be invalid due to a malfunction. A photomicrograph appears in Figure 24 and indicates non-spherical aerosol particles. The experimental response was much lower than predicted. This may be due to aerosol shape and variations from a log normal size distribution. There is also evidence that the aerosol contained water which evaporated as the filter samples were gathered. The above problems indicate high uncertainty in this data.

EXPERIMENTAL DATA LOG

SET: 2 **TEST:** 1 **DATE:** 7/18/75

AEROSOL MATERIAL: 0.5 μm PSL

MEASURED OPACITY: 13.8%

SIZE DISTRIBUTION: Determined by counting.

VOLUME MEDIAN DIA.: $0.75\ \mu m\ ^{+0.2}_{-0.16}$

GEOMETRIC STD. DEV.: $2.0\ ^{+0.8}_{-0.6}$

MEASURED MASS CONCENTRATION (by filter) (mg/m^3):

INLET: 14.1 and 14.5

OUTLET: 13.8 and 13.8

NEBULIZER AND PRESSURE: Collison @ 20 psi

NEBULIZER FLUID CONCENTRATION: 1/4%

SIZE CALCULATED FROM OPACITY AND MASS MEASUREMENTS: Opacity corresponds to a VMD of 0.7 and geometric standard deviation of 2.0.

PHOTOMICROGRAPH MEASUREMENTS:

Diameter (μm)	Cumulative % by Weight	No. of Particles or Agglomerates
0.5 (Singlets)	31	15
0.63 (Doublets)	38	4
0.72 (Triplets)	49	4
7-1	57	2
1-1.3	100	4
1.3-1.8	100	0

COMMENTS: An SEM photomicrographs of the aerosol were taken; the counting statistics are shown above. There was very good agreement among measurements and theory.

EXPERIMENTAL DATA LOG

SET: 2 **TEST:** 2 **DATE:** 7/21/75

AEROSOL MATERIAL: 0.5 μm PSL

MEASURED OPACITY: 20%

SIZE DISTRIBUTION:

VOLUME MEDIAN DIA.: $0.75\mu m\ ^{+0.14}_{-0.12}$

GEOMETRIC STD. DEV.: $1.7\ ^{+0.4}_{-0.3}$

MEASURED MASS CONCENTRATION (by filter) (mg/m^3):

INLET: 19.6 and 19.6

OUTLET: 20.3 and 21.2

NEBULIZER AND PRESSURE: Collison @ 18 psi

NEBULIZER FLUID CONCENTRATION: 1/2%

SIZE CALCULATED FROM OPACITY AND MASS MEASUREMENTS: Excellent agreement between measured opacity and size distribution.

PHOTOMICROGRAPH MEASUREMENTS:

Diameter (μm)	Cumulative % by Weight	No. of Particles or Agglomerates
0.5 (Singlets)	15	21
0.63 (Doublets)	39	17
0.72 (Triplets)	51	6
.7-1.	73	5
1.-1.3	90	2
1.3-1.8	100	1
1.8-2.3	100	0

COMMENTS: Size distribution determined by counting SEM photomicrographs, one of which is shown in Figure 21. The counting statistics appear above. There was very good agreement between theoretical and experimental results.

EXPERIMENTAL DATA LOG

SET: 2 **TEST:** 3 **DATE:** 7/15/75

AEROSOL MATERIAL: 2.02 μm PVL

MEASURED OPACITY: 8.2%

SIZE DISTRIBUTION:

VOLUME MEDIAN DIA.: 2 μ

GEOMETRIC STD. DEV.: See below.

MEASURED MASS CONCENTRATION (by filter) (mg/m^3):

INLET: 36.3 and 32.1

OUTLET: 30.0 and 29.7

NEBULIZER AND PRESSURE: Collison @ 17.5 psi

NEBULIZER FLUID CONCENTRATION: 1.5%

SIZE CALCULATED FROM OPACITY AND MASS MEASUREMENTS: Good agreement with optical measurement.

PHOTOMICROGRAPH MEASUREMENTS: Particles counted optically as shown below.

	Inlet		Outlet	
	% by Volume	No. Counted	% by Volume	No. Counted
Singlets	56	220	60	151
Doublets	21	41	30	38
Triplets	10	13	8	7
Quads	5	5	2	1
Agglomerate	8	3	0	0

COMMENTS: Scatometer response was higher than for Set 1 2 μm aerosols. Lower experimental response than predicted is perhaps due to high number of doublets but more likely an artifact of the rapid variation in light scattering at this size which is not compensated for in the theoretical calculations.

EXPERIMENTAL DATA LOG

SET: 2 TEST: 4 DATE: 7/15/75

AEROSOL MATERIAL: 2.02 μm PVL

MEASURED OPACITY: 13.2%

SIZE DISTRIBUTION: Determined by counting.

VOLUME MEDIAN DIA.: 2 μ

GEOMETRIC STD. DEV.: See below.

MEASURED MASS CONCENTRATION (by filter) (mg/m^3):

INLET: 57.6 and 59.3

OUTLET: 57.9 and 58.4

NEBULIZER AND PRESSURE: Collison @ 30 psi

NEBULIZER FLUID CONCENTRATION: 3%

SIZE CALCULATED FROM OPACITY AND MASS MEASUREMENTS: Opacity corresponded to particles somewhat larger than 2 microns.

MICROSCOPE MEASUREMENTS: Particles counted optically are shown below:

	% by Volume	No. of Particles
Singlets	54	159
Doublets	20	30
Triplets	17	17
Quads	4	3
Agglomerates	5	2

Outlet showed similar size distribution.

COMMENTS: Mass concentration calculated using opacity and assuming 2 micron spheres was 13 percent lower than true value; the difference is likely due to agglomeration. The experimental response was considerably lower than theoretical prediction. Again this is likely due to problems in calculating theoretical response.

EXPERIMENTAL DATA LOG

SET: 2 TEST: 5 DATE: 7/20/75

AEROSOL MATERIAL: 5.7 μm PSL

MEASURED OPACITY: 8.1%

SIZE DISTRIBUTION: Determined by counting.

VOLUME MEDIAN DIA.: 5.7 μ

GEOMETRIC STD. DEV.: See below.

MEASURED MASS CONCENTRATION (by filter) (mg/m^3):

INLET: 102 and 100

OUTLET: 76 and 75

NEBULIZER AND PRESSURE: Retec X-70/N @ 30 psi

NEBULIZER FLUID CONCENTRATION: 5%

SIZE CALCULATED FROM OPACITY AND MASS MEASUREMENTS: Opacity agrees well with observed size distribution.

MICROSCOPE MEASUREMENTS:

	Inlet		Outlet	
	% by Volume	No. Counted	% by Volume	No. Counted
Singlets	80	102	85	137
Doublets	20	26	11	18
Triplets	0	0	4	2

A small amount of preferential settle out appears to have occured; however, it is of little overall consequence.

COMMENTS: Agreement between measured and calculated opacity is good. The mass concentration in the beam was taken to be the average of the inlet and outlet as the fallout was not as great at the Set 1 test. The calculated mass concentration based on opacity was 6 percent higher, almost exactly midway between the inlet and outlet average and inlet concentration. Higher flowrates and a more monodisperse aerosol contributed to the lower fallout compared to Set 1.

EXPERIMENTAL DATA LOG

SET: 2 **TEST:** 6 **DATE:** 7/23/75

AEROSOL MATERIAL: Ammonium fluorescein

MEASURED OPACITY: 14%

SIZE DISTRIBUTION: Determined by impactor (4 samples)

VOLUME MEDIAN DIA.: $0.57\ \mu m\ ^{+0.12}_{-0.10}$

GEOMETRIC STD. DEV.: $2.1\ ^{+0.4}_{-0.4}$

MEASURED MASS CONCENTRATION (by filter) (mg/m^3):

INLET: 10.7 and 13.9

OUTLET: 13.5 and 12.2

NEBULIZER AND PRESSURE: Retec X-70/N @ 22.5 psi

NEBULIZER FLUID CONCENTRATION: 0.4%

SIZE CALCULATED FROM OPACITY AND MASS MEASUREMENTS: Opacity is in agreement with measured size.

MICROSCOPE MEASUREMENTS: An SCM photomicrograph appears in Figure 23.

COMMENTS: Adequate agreement between theory and measured data in this experiment. Large uncertainty in mass concentration, ±12% (95% confidence) results in large uncertainty in estimating size distribution.

EXPERIMENTAL DATA LOG

SET: 2 **TEST:** 7 **DATE:** 7/24/75

AEROSOL MATERIAL: Ammonium Fluorescein

MEASURED OPACITY: 23%

SIZE DISTRIBUTION: Determined by four impactor samples.

VOLUME MEDIAN DIA.: $2.84\ \mu m\ ^{+1.2}_{-0.6}$

GEOMETRIC STD. DEV.: $3.7\ ^{+0.6}_{-0.6}$

MEASURED MASS CONCENTRATION (by filter) (mg/m^3):

INLET: 83.7 and 87.0

OUTLET: 84.3 and 87.3

NEBULIZER AND PRESSURE: Retec X-70/N @ 10 psi

NEBULIZER FLUID CONCENTRATION: 9%

SIZE CALCULATED FROM OPACITY AND MASS MEASUREMENTS: Somewhat larger size distribution indicated than impactor and SEM measurements.

MICROSCOPE MEASUREMENTS: A SEM photo of this aerosol is shown in Figure 25. Note large hollow spheres which likely contained some water while in the scattering chamber. The size distribution differs significantly from a log normal; a cut off at about 5 microns in diameter is indicated by the impactor measurements.

COMMENTS: The odd size distribution makes comparison with theory uncertain. A fair amount of water may have been present in hollow spheres during Scatometer measurements and it is likely that this water evaporated to a large extent during filter sampling (aerosol RH was 25-30%). Further drying of filter samples resulted in a 6% weight loss. Problems were also encountered with the nephelometer during this run. As in Set 1, it is uncertain whether the low response is due to light scattering or experimental problems.

APPENDIX B

DATA REDUCTION COMPUTATIONS

Several steps are necessary to calculate Scatometer aerosol concentrations for comparison to actual concentrations determined from gravimetric filter measurements. In practice, all scattering intensities were power measurements because the detector measured the power received through its aperature: these intensities will be denoted using the letter P.

Step 1) Normalize each intensity, $P(\theta)$, to a constant beam strength, P_{BN}. This procedure corrects the measured intensities for changes in the beam power.

$$P_N(\theta) = P(\theta)\frac{P_{BN}}{P_B} \qquad (B1)$$

P_B = beam power during measurement

P_{BN} = the reference beam power

$P_N(\theta)$ = intensity normalized to the reference strength

Step 2) Calculate the transmittance, T_i, and optical depth, O_i. The transmittance is measured twice during each experiment and i equals one or two.

$$T_i = \frac{P_N(0)}{P_{NO}(0)}$$

$$O_i = \ln T_i \qquad (B2)$$

$P_N(0)$ = normalized beam power with aerosol at 0° (beam focal point)

$P_{NO}(0)$ = normalized beam power without aerosol at 0°

Step 3) Correct T_i and O_i to a reference aerosol concentration.

$$O_{Ni} = O_i \frac{b_N}{b_i} \tag{B3}$$

$$T_{Ni} = \exp(O_{Ni})$$

b_N = reference relative aerosol concentration (normally based on the average aerosol scattering coefficient during the test)

b_i = aerosol scattering coefficient during intensity measurement

O_{Ni} = normalized optical depth

T_{Ni} = normalized transmittance

Step 4) Compute reference optical depth, $O_{N'}$ transmittance, T_N and error

$$O_N = \left(O_{N1} + O_{N2}\right)/2 \tag{B4}$$

O_N is the reference optical depth for the aerosol. All scattering intensities are corrected to the same relative aerosol density using $b_{N'}$ and will correspond to the scattering at this optical depth. The error in determining O_N is taken as the standard deviation of O_{N1} and O_{N2}. This error includes that introduced by the nephelometer. Note that the nephelometer does not measure absolute aerosol mass concentration accurately; however, since size distributions are nearly constant, it does provide an accurate measure of relative mass concentration.

Step 5) Correct scattering intensities to reference relative aerosol concentration and correct for attenuation by aerosol

$$P_{Ni}(\theta) = P_i(\theta) \frac{b_N}{b_i} \left[\exp(-O_n b_i / b_N)\right]^{-1} \quad \text{(B5)}$$

b_i = relative density during $P_i(\theta)$ measurement

Note that $\exp(-O_N b_i / b_N)$ is the transmittance for the aerosol density corresponding to b_i. $P_i(\theta) \frac{b_N}{b_i}$ is the scattered power corresponding to b_N.

Step 6) Compute average normalized scattering, $P_N(\theta)$, at angle θ and error.

$$P_N(\theta) = (P_{N1} + P_{N2})/2 \quad \text{(B6)}$$

The error in $P_N(\theta)$ is estimated as the standard deviation of P_{N1} and P_{N2}.

Step 7) Correct aerosol mass concentrations determined from filter measurements to the reference relative concentration, b_N, and determine the average if multiple measurements are taken.

$$M_{Ni} = M_i \frac{b_N}{b_i} \quad \text{(B7)}$$

M_i = absolute mass concentration determined by aerosol filtration

M_{Ni} = aerosol mass adjusted to constant relative concentration

b_i = average nephelometer readout during measurement period, 3 to 8 minutes

At this point all scattering, transmittance, and aerosol concentration measurements have been corrected to the same aerosol concentration. The Scatometer mass concentrations are calculated in Step 8 and 9 for direct comparison with the filter measurements which are the true absolute aerosol concentrations. These normalizations are necessary since all measurements cannot be made simultaneously.

Step 8) Calculate Scatometer aerosol volume concentration, $V_c(\theta)$, versus angle.

$$V_c(\theta) = 0.224 \sqrt{O_N \, P'_N(\theta)/P_{BN}} \, cm^3/m^3 \qquad (B8)$$

$$P'N(\theta) = P_N(\theta)/R(\theta)$$

$R(\theta)$ = active volume ratio at angle θ

This formula, (B8), has been derived from Equation (10): O_N is directly proportional to the aerosol cross section and $P'_N(\theta)/P_{BN}$ to the scattering cross section. The constants of proportionality are grouped into the 0.224 constant. More explicity, $V_c(\theta)$, is given by

$$V_c(\theta) = V(\theta)/A_b L \qquad (B9)$$

where $V(\theta)$ = aerosol volume in Scatometer beam

A_b = beam area

L = length of scattering chamber

and $A_b L$ = volume of scattering beam

Notice that the Scatometer measures the total volume in its beam, $V(\theta)$. $V(\theta)$ from Equation (10) is

$$V(\theta) = \frac{4}{3} \pi \frac{2}{k} \frac{1}{\sqrt{\pi Q_o}} \sqrt{\sigma(\theta)\, \sigma_e} \qquad \text{(B10)}$$

and

$$\sigma(\theta) = \frac{P_N(\theta)}{\pi\ P_{BN}\ R_A(\theta)}\ A_b \left(\frac{r_f}{r_d}\right)^2 \qquad \text{(B11)}$$

$k = 2\pi/\lambda$

r_f = focal length of focusing lens = 641.6 mm

r_d = radius of detector aperture = 1.04 mm

λ = wavelength

$\sigma_e = O_N\ A_b$

Note that the active volume ratio corrects the scattering intensity for light scattered by the aerosol which is not collected by the final lens.

Substituting into Equation (B10), $V(\theta)$ is given as

$$V(\theta) = \frac{4}{3} \frac{\lambda}{\pi} \frac{1}{Q_o}\ A_b \frac{r_f}{r_d} \sqrt{O_N \frac{P_N(\theta)}{P_{BN}\ R(\theta)}} \qquad \text{(B12)}$$

The constants to the left of the square root are lumped into the 0.224 constant in Equation (B8).

Step 9) Calculate Scatometer mass concentration, $M_s(\theta)$

$$M_s(\theta) = \rho\ V_c(\theta) \qquad \text{(B13)}$$

ρ = aerosol specific gravity

The values $M_s(\theta)$ may now be directly compared to the absolute mass concentrations based on filter sampling.